Fermi National Accelerator Laboratory

FN-491
[SSC-180]

Minimum Propagating Zone of the SSC Superconducting Dipole Cable

King-Yuen Ng
SSC Central Design Group
c/o Lawrence Berkeley Laboratory 90/4040
Berkeley, California 94720
and
Fermi National Accelerator Laboratory
P.O. Box 500, Batavia, Illinois 60510

August 1988

Operated by Universities Research Association Inc. under contract with the United States Department of Energy

SSC-180
FN-491

MINIMUM PROPAGATING ZONE OF THE SSC SUPERCONDUCTING DIPOLE CABLE

King-Yuen Ng

*SSC Central Design Group**

c/o Lawrence Berkeley Laboratory 90/4040, Berkeley, CA 94720

and

*Fermi National Accelerator Laboratory**

Batavia, IL 60510

(August 1988)

*Operated by the Universities Research Association, Inc., under contracts with the U.S. Department of Energy.

I. INTRODUCTION

When an amount of energy is deposited on a superconducting cable, the first reaction is a local rise in temperature and a drop in critical current density. The superconductor may not be able to carry all the operating current and part of it sees a resistivity and sets up a potential along the cable. Further heat will be generated with a further increase in temperature. This cascade can eventually lead to a quench, unless this heat can be conducted away rapidly or sufficient cooling is provided. Thus, a cable made up of purely superconducting material is highly unstable. A practical superconducting cable contains many strands, each of which consists of a matrix of superconducting filaments embedded in copper. Having a much lower resistivity than superconductor in the normal phase, the copper will carry most of the excess current and set up a much lower potential along the cable. As a result, the heat generation will be very much reduced. Also, having a much higher thermal conductivity than the superconducting material, the excess heat can be conducted away more efficiently along the cable and to the surface of the cable to be cooled by the surrounding helium bath. If the amount of energy deposited on the cable is small, the disturbance will subside. On the other hand, if the amount of energy deposited is big, the disturbance will grow along the cable and we have a quench.

There are two types of disturbances. A point disturbance is an amount of heat deposited on a very *short* length of the cable. The quenching of the cable is caused by the spreading of the disturbance. On the other hand, a distributed disturbance is referred to as heat added rather uniformly on a big length of the cable. The effects of the latter are generally well understood and should not cause any serious problems if they are fully taken into account at the design stage. Here, we are dealing with point disturbances only. We hope to compute the minimum amount of heat in a point disturbance that will start a quench. Obviously, the amount of heat required to quench a strand will depend on the copper-to-superconductor ratio in the strand, the copper resistivity, the copper thermal conductivity, and the heat transfer coefficient at the strand's surface. A knowledge of these dependencies will definitely be beneficial to the design of a superconducting cable.

The above problem involves the solution of a time-dependent heat flow equation. The result will depend critically on the initial condition or how the amount of heat is deposited onto the cable, for example, the time duration of the heat deposition and its distribution along the cable. The steady-state solution is much simpler. But it is of not much help. This is because heat is constantly generated in the cable strand and it takes a long time for an equilibrium steady state to establish. As a result, the energy contained in the steady-state solution may be very much larger than the

energy in the original point disturbance and therefore does not reflect the minimum energy required to start a quench at all. In the absence of surface cooling, nontrivial steady-state solution does not even exist for an infinitely long one dimensional cable.

We have studied the time evolution of a concentrated disturbance. If the initial energy of the disturbance is small, the disturbance temperature profile spreads out, approaches a critical temperature profile slowly, and subsides eventually as shown in Fig. 1(a). If the energy in the disturbance is big enough, the disturbance also spreads out until it reaches a critical profile. After that, however, the temperature rises everywhere resulting in a quench as shown in Fig 1(b). In both cases, no nontrivial steady state has been reached. These results inspire us to study *propagating* solutions instead. They are heated zones whose temperature grows at all points along the cable. The propagating solution which contains the least energy is called the minimum propagating zone (MPZ).[1] In Section III, these propagating zones are approximated using the steady-state heat flow equation. We find that the energy in the approximate MPZ gives the correct order-of-magnitude estimate to the minimum energy required to cause a quench.

In Section II, we list and define all the input information required in the heat flow equation. The results of the computation are discussed in Section IV. Finally, in Section V, some remarks and conclusions are given.

II. INPUT INFORMATION

This computation was performed specially for the superconducting cable of the Superconducting Super Collider (SSC) dipoles (the C358A Cross Section), although it can be applied to other cable as well.[2] Some preliminary results have been reported in Ref. 3.

II.1 Maximum magnetic field seen by cable

A strand of the C358A Cross Section cable has

$$\begin{aligned} \text{radius } a &= 0.404 \text{ mm} \\ \text{number of superconductor filaments } N &\cong 11000 \\ \text{copper-to-superconductor ratio } r &= 1.3 \ . \end{aligned}$$

For the inner coil of the dipole, there are $S = 23$ strands in the cable which carry a total operating current of $I_{\rm op} \cong 6.5$ kA at bath temperature $\theta_0 \cong 4.2$ K. The magnetic flux density B_0 at the center of the beam pipe is given by

$$B_0 = f(I_{\rm op}) I_{\rm op}. \tag{2.1}$$

The maximum magnetic field $B_{\max}$ seen by the cable is usually in the inner part of the extreme bottom or top turn of the coil. It is related to B_0 by

$$B_{\max} = m(I_{\rm op})B_0. \tag{2.2}$$

In above, the transfer function $f(I_{\rm op})$ and the maximum flux ratio $m(I_{\rm op})$ depend, for a magnet design, on the geometry of the coils, collars, and yoke, and the magnetic properties of the materials. For C358A, they are supplied by Wanderer:[4]

$$f(I) = \frac{1.1372 - 0.01861I}{1 + 0.045\exp(-0.00235I^4)} ,$$

$$m(I) = 1.0490 + 0.00107(I - 5.5)\left[1 - e^{-1.56(I-5.5)}\right] ,$$

where the current I is in kA.

II.2 Thermodynamic surface for NbTi material

The maximum current that can flow in a superconducting cable of the C358A Cross Section at temperature θ with transverse magnetic flux density B in the superconducting phase has been measured by Morgan[5] and is given by

$$I_c(B,\theta) = I_c({\rm SP})\left(1 + \frac{P_2u + P_3u^2 + P_4u^3}{1 + P_5v}\right)\left(\frac{1 + P_6v}{1 + P_7v + P_8v^2}\right) , \tag{2.3}$$

where $u = \theta - 4.2$ in K, $v = B - 5.0$ in teslas, $P_2, \ldots, P_8 = -0.35424$, -0.023346, 0.0061392, -0.15335, -0.2108, 0.0065461, -0.016687, respectively, $I_c({\rm SP}) = 13.39$ kA is the critical current in the cable consisting of $S = 23$ strands at 4.2 K and 5.0 teslas.

The performance of superconducting wires usually falls short of what might have been expected from the results on short samples of the material. This effect is known as "coil degradation." In Morgan's measurement, the degradation was $D \sim 0.05$. There, the critical current density of NbTi is

$$j_c(B,\theta) = \frac{I_c(B,\theta)}{\lambda SA(1 - D)} , \tag{2.4}$$

where $A = \pi a^2$ is the cross sectional area of a strand, and

$$\lambda = \frac{1}{1 + r} \tag{2.5}$$

is the fraction of superconductor in the strand. Equation (2.4) is called the thermodynamic surface of the NbTi material in the cable; it separates the superconducting phase from the normal phase.

In operation, of course, all the current will flow in the superconductor filaments only. The current density in the filaments $j_{\rm op}$ is therefore given by

$$I_{\rm op} = \lambda S A j_{\rm op} \ . \tag{2.6}$$

As an example, at operation current $I_{\rm op} = 6.5$ kA and copper-to-superconductor ratio $r = 1.3$, $j_{\rm op} = 1.27 \times 10^9$ A/m^2. The magnetic flux density at the center of the beam pipe is, from Eq. (2.1), $B = 6.6015$ T. Then, the maximum magnetic flux density seen by the cable is, from Eq. (2.2), $B_{\rm max} = 6.9305$ T. The thermodynamic curve, given by Eq. (2.3) at $B_{\rm max}$, separating the superconducting phase and the normal phase is shown in Fig. 2. There, we have also plotted the point of operation at $\theta_0 = 4.2$ K. The critical current density at $\theta = 4.2$ K is found to be $j_c = 1.71 \times 10^9(1-D)$ A/m^2, where D is the coil degradation.

II.3 Heat generation

Below, we shall deal with the superconducting cable at maximum magnetic flux density $B_{\rm max}$, because the critical current density is smallest there. When the temperature is raised to $\theta > \theta_g$ (Fig. 2), the critical current density $j_c(\theta) = j_c(B_{\rm max}, \theta)$ or the maximum current density that can be carried by the NbTi in the superconducting phase is less than $j_{\rm op}$. The leftover current $\lambda A[j_{\rm op} - j_c(\theta)]$ (for a strand) has to flow either in the copper or the NbTi filaments in the normal state. However, since NbTi in the normal state has a resistivity of $\rho_{sc} \cong 6.5 \times 10^{-7}$ Ωm at $\sim$7 T and 4.2 K, which is very much bigger than that of copper $\rho_{cu} \cong 3 \times 10^{-10}$ Ωm, nearly all of this leftover will flow in the copper setting up along the strand an electric field

$$E = \frac{\lambda}{1-\lambda} \rho_{cu} [j_{\rm op} - j_c(\theta)] \ . \tag{2.7}$$

Of course, a tiny amount of the leftover current will flow in the NbTi filaments so that the potential drop along the NbTi filaments will be the same as that along the copper. The total current will now see a potential and heat will be generated. The generation per unit volume is

$$G(\theta) = \lambda j_{\rm op} E \ , \tag{2.8}$$

where the factor λ comes in because the total current is designed to flow in the NbTi filaments only [see Eq. (2.5)]. Note that the heat generation is equal to the *total* current but not just the leftover multiplied by the potential drop, because the potential is experienced by the total current.

We now make the assumption that the thermodynamic curve separating the two phases of NbTi in Fig. 2 is a straight line intercepting the temperature axis at θ_c,

which is the temperature above which NbTi becomes completely normal no matter how small the current is. Then, the critical current density $j_c(\theta)$ can be expressed in terms of the operation current density $j_{\rm op}$ by

$$j_c(\theta) = \frac{\theta_c - \theta}{\theta_c - \theta_g} j_{\rm op} \ , \tag{2.9}$$

and, from Eqs. (2.7) and (2.8), the generation per unit volume becomes

$$G(\theta) = \frac{\lambda^2 \rho_{cu} j_{\rm op}^2}{1-\lambda} \frac{\theta - \theta_g}{\theta_c - \theta_g} \qquad \text{when } \theta_c > \theta > \theta_g. \tag{2.10}$$

Obviously, Eq. (2.10) will apply only when $\theta_g < \theta < \theta_c$. Above θ_c, NbTi is completely in the normal phase and practically all the current will flow in the copper. The generation will reach the maximum

$$G_c = G(\theta_c) = \frac{\lambda^2 \rho_{cu} j_{\rm op}^2}{1-\lambda} \qquad \text{when } \theta > \theta_c, \tag{2.11}$$

and will not increase further at higher temperatures except for the temperature dependence of ρ_{cu} on θ. The generation curve is plotted in Fig. 3.

II.4 Surface cooling

The heat on the superconducting strand will be transferred across the surface of the strand to adjacent strands or helium with a bath temperature of θ_0. The rate at which heat is transferred per unit length is given by $PH(\theta)$, where P is the perimetric circumference of the strand. For a single strand, $P = 2\pi a$, where a is the radius of the strand.

We assume that the cooling is proportional to the temperature difference between the cable and the surrounding bath, or

$$H(\theta) = h(\theta - \theta_0) \ , \tag{2.12}$$

where h is called the heat transfer coefficient and is assumed to be time and temperature independent. For cooling by nucleate pool boiling of He, $h \sim 5 \times 10^4$ wm^{-2}K^{-1}. Usually, there is only about 5% of helium inside a composite cable, and this helium does not flow very freely between the strands. In the situation of a disturbance in a strand, the excess heat is mostly conducted to the adjacent strands rather than cooled by the stagnant helium. The cable is wrapped around with a layer of insulation which has a typical thickness of $w \sim 50$ to 250 μm and a typical thermal conductivity of

$k \sim 5 \times 10^{-2} \mathrm{wm}^{-1}\mathrm{K}^{-1}$. This gives a surface heat transfer coefficient of $h = k/w = 200$ to 1000 $\mathrm{wm}^{-2}\mathrm{K}^{-1}$. Experimental measurement gives a value of $h \sim$1500 $\mathrm{wm}^{-2}\mathrm{K}^{-1}$.

As a result, it may not be suitable to talk about the surface cooling of one strand alone. We may take the cable as a whole, which contains $S = 32$ strands arranged in two rows. Area of cable is $A \sim S\pi a^2$, whereas the perimetric circumference is $P \sim 4a(S/2 + 2)$. Therefore, roughly $P/A \sim 2/\pi a$. Each turn of the cable is piled with the broad side one upon the other so that only the narrow sides, total length $8a$, are in contact with liquid helium. Then, $P/A \sim 8/S\pi a$. We are not so sure which value of P/A should be used. In the computation below, however, we shall use $P/A = 2/a$. Results for other values of P/A can be obtained by scaling h.

II.5 Electric resistivity of copper

The resistivity of copper is a function of temperature θ and magnetic flux density B. It also depends on the purity of copper. An experimental measurement gives for bulk copper below $\sim$ 10 K,

$$\rho_{cu}(\theta, B) = \left(0.0032\, B + \frac{1}{\mathrm{RRR}}\right) \times 1.7 \times 10^{-8}\ \Omega\mathrm{m}\ , \tag{2.13}$$

where B is in tesla. The first term is called the magneto-resistivity and the residual resistivity ratio (RRR) in the second term is a measure of copper purity. We note that when $B_{\max} \sim 7$ T, magneto-resistivity will dominate when RRR $\gtrsim 45$.

II.6 Thermal conductivity of copper

The thermal conductivity is related to its resistivity. For a fair approximation, it obeys the Wiedemann-Franz law[6]

$$k\rho_{cu} = L_0\theta\ , \tag{2.14}$$

where the Lorentz number $L_0 = \pi^2 k_B^2/3e^2 = 2.45 \times 10^{-8}\ \mathrm{w}\Omega\mathrm{K}^{-2}$ with k_B the Boltzmann's constant and e the electronic charge. Thus, the thermal conductivity is affected by magnetic flux as well as purity. At low temperature, it is linear in θ. However, in our computation below, we shall consider k as a constant for the sake of simplicity and take $k \sim 350$ w/mK. This assumption is not so bad because, as shown in Section IV.2 below, the temperature variation in the MPZ is $\sim$ 2 K only.

The thermal conductivity of NbTi at cryogenic temperatures in a magnetic flux density of 6 T is 0.1 w/mK, which is negligible compared with that of copper. Therefore, in a strand, the heat generated in some portions of the superconducting filaments

is first transferred to the surrounding copper and then conducted away through the copper. With copper content of $(1-\lambda)$ in the strand, the effective thermal conductivity longitudinally along the strand should be $(1-\lambda)k$. This fact has not been taken into account in Ref. 2.

II.7 Specific heats of copper and NbTi

In computing the heat required to set up a heated zone, we take at $\theta_r = 4.2$ K

$$\begin{aligned} \text{volume specific heat of Cu } C_{cu} &= 1.6 \times 10^3 \text{ j/m}^3\text{K} \\ \text{volume specific heat of NbTi } C_{sc} &= 6.8 \times 10^3 \text{ j/m}^3\text{K} \end{aligned}$$

and assume that they vary according to θ^3 at cryogenic temperatures. For the copper-NbTi complex, we can therefore define an effective specific heat

$$C_{\text{eff}}(\theta) = [\lambda C_{sc} + (1-\lambda)C_{cu}] \left(\frac{\theta}{\theta_r}\right)^3 . \tag{2.15}$$

III. DERIVATION OF PROPAGATING ZONES

III.1 The heat flow equation

We assume that the strand is narrow enough so that uniform thermal distribution can be established easily across the strand. Thus, we need to study the temperature profile along the strand in the z-direction only. The latter is determined by the one-dimension heat flow equation

$$C_{\text{eff}}(\theta) A \frac{\partial \theta}{\partial t} = \frac{\partial}{\partial z}\left[k(1-\lambda)A\frac{\partial \theta}{\partial z}\right] + AG(\theta) - PH(\theta) , \tag{3.1}$$

where A and P are the cross sectional area and perimetric circumference of the strand, and $G(\theta)$ and $H(\theta)$ are the heat generation and surface cooling given by Eqs. (2.10) to (2.12). The factor $(1-\lambda)$ on the right side reminds us that only the copper portion of the strand will conduct heat with a thermal conductivity k.

In general, the heated temperature profile consists of three zones bounded by $z = z_c$, z_g, z_0 where the temperatures are at $\theta = \theta_c$, θ_g, θ_0 respectively. Or

region 1:	$\theta > \theta_c$	constant generation Eq. (2.11) + surface cooling
region 2:	$\theta_c > \theta > \theta_g$	linear generation Eq. (2.10) + surface cooling
region 3:	$\theta_g > \theta > \theta_0$	only surface cooling

We now discuss the transience. For simplicity, the surface cooling term $PH(\theta)$ is dropped. When a concentrated disturbance occurs at $z \sim 0$, the first term on the right of Eq. (3.1), *i.e.,* the second derivative with respect to z, dominates as a result of the concentration, and is negative at the center and positive at the edge. Therefore the temperature at the center drops and that at the edges rises resulting in a spreading out of the disturbance. As the spread progresses, the second derivative with respect to space becomes smaller and the heating effect of the second term $AG(\theta)$ becomes more significant. Except near a steady state, equilibrium will be reached in regions 1 and 2 roughly in time of the order

$$\tau_c = \frac{4C_{\text{eff}} z_g^2}{\pi^2(1-\lambda)k} , \tag{3.2}$$

where z_g is the half width of the generation region (or $z = z_g$ when $\theta = \theta_g$). The derivation is given in Section III.2 below. For $I_{\text{op}} = 6.5$ kA and copper-to-superconductor ratio 1.3, $z_g \sim 1.59$ mm, or $\tau_c \sim 30$ μs. By equilibrium, we mean that heat generation is balanced by heat conduction at all points inside the regions with generation. There are many equilibrium solutions just for regions 1 and 2. Which one the disturbance will arrive at depends on the size of the initial disturbance. At this point, the temperature profile continue to adjust itself so as to reach a steady-state solution for all the three regions. If the energy in this temperature profile is small, it will continue to flatten out and collapse eventually as shown in Fig. 1(a). If the energy is too big, it will propagate outward with temperature rise at all points and diverge as shown in Fig. 1(b). If the energy is just right, the temperature profile will reach a nontrivial steady state, provided that such a steady state exists. In this case, the the time to reach the steady-state profile will be infinite. The evolutions of the peak temperature corresponding, respectively, to Fig. 1(a) and Fig. 1(b) are plotted in Fig. 4(a) and Fig. 4(b). Alongside, the evolutions of the energy stored in the profiles are also plotted. Here, in either Figs. 4(a) or 4(b), the time to reach the intermediate equilibrium state is rather long. This is because this equilibrium state is very near to the steady-state solution for the whole composite strand, which exists even without surface cooling since a finite length of the strand (20 cm) has been used in the numerical computation. Even if the intermediate temperature profile is not near a steady state, a lot of the evolution time is spent in approaching it. For this reason, this intermediate temperature profile is a critical temperature profile.

Does the critical temperature profile depend on the shape and width of the original disturbance? The answer is yes, but not much if the original disturbance is sufficiently concentrated. The reason is that the time taken to approach the critical temperature profile is very much longer than the time taken by the disturbance to spread out, as depicted in Figs. 4(a) and (b). In fact, assuming a narrow gaussian disturbance,

the rate at which the peak temperature drops is $d\theta_p/dt \propto -\theta_p^6$. Therefore, if the disturbance is made more concentrated, the amount of heat generated during this additional spread-out time will be extremely small. For example, we have reduced the widths of the disturbances in Figs. 1(a) and (b) from 0.2 mm by 10 times and 100 times but keeping the energy constant. The changes in energies of the corresponding critical temperature files are extremely small. We have also changed the shape of the disturbance from a gaussian to the shape of a cosine. But essentially the same critical temperature profile is reached. This leads us to believe that if we trace each critical temperature profile backward in time, the energy of the disturbance should tend to a limit when the width of the disturbance goes to zero.

Thus, for a point deposition of a certain energy, there exists a unique critical temperature profile which is in equilibrium in the regions with generation. This critical temperature profile determines whether the future evolution will diverge or subside. In the case of future divergence, this critical temperature profile is called a critical propagating temperature profile or zone. A family of such critical propagating temperature profiles are therefore generated by varying the initial energy deposition. Each critical propagating temperature profile contains a certain amount of energy. If we start from a point disturbance of a high energy, the energy in the resulting propagating profile will definitely be large. On the other hand, the energy of the propagating profile is also large if we start from a point disturbance with a relatively low energy. This is because this critical prpagating profile becomes very near to the steady-state solution. It takes a long time for the disturbance to approach the profile, and a lot of heat will be generated in the process. Thus, in between there should be a critical propagating profile which contains the least amount of energy, and this critical propagating profile is defined as the minimum propagating zone (MPZ) corresponding to an initial point deposition. The time evolutions of the peak temperature and energy of the point deposition corresponding to the MPZ are shown in Fig. 5. The temperature profile of the MPZ is shown in Fig. 7 in dashes.

We would like to point out that our definition of MPZ is quite different from the usual one.[1] Usually, one defines the MPZ as the steady-state solution and the energy is taken as the energy stored in the generation region only, *i.e.*, for $z < |z_g|$, but not the total energy in the solution, because the latter may go to infinity for a cable of infinite length. A MPZ defined in this way will depend critically on the amount of surface cooling. It will be shown in Section IV.5 below that heat removal through surface cooling is very much slower than through copper conduction. But without cooling, there will not be any nontrivial steady state for a one-dimensional strand of infinite length, and a MPZ cannot be defined. Therefore, we think our definition of the MPZ is much better.

III.2 Propagating solutions

The exact analytic solution of the time dependent heat flow equation appears to be out of the question, because the equation is *not* linear. Thus, we need to follow the time evolution numerically to see whether a certain energy of point deposition will cause a quench. This has to be done many times until the minimum energy required to start a quench can be determined. This process is undoubtedly very time consuming. Another way is to derive the MPZ mentioned above. The energy it contains will give roughly the minimum energy to start a quench. This is because the evolution time $\sim \tau_c$ from the initial point deposition to the MPZ is not too big and the heat generated during the evolution will not be too big also. Unfortunately, exact analytic solutions for the above mentioned propagating zones also appear impossible. Instead, we try to look for simple analytic solutions that can approximate these propagating zones. These approximate solution must grow at all points along the cable strand as time evolves, or it must propagate outward and diverge. From the previous subsection, we know that the exact propagating profiles are in equilibrium in regions 1 and 2. Therefore the approximate solutions that we are looking for can be constructed from solving the *steady-state* heat flow equation with the temperature gradient continuous everywhere except at the point $\theta = \theta_0$, or the very edge of the zone. One of these solutions is shown in Fig. 6. Since this solution satisfies the steady-state heat flow equation everywhere except at the end points, temperature will rise only at these points. As time evolves, the temperature rise at the end points will spread out and there will be a gradual temperature rise at all points. This is demonstrated in Fig. 6 by the dashed curves. Therefore, this solution constitutes a propagating zone.

Let us solve for such a solution analytically under the simple situation that the temperature does not exceed θ_c and there is no surface cooling. Then, there are only regions 2 and 3. The solution in region 2 is

$$\theta - \theta_g = (\theta_p - \theta_g)\cos\alpha z \ , \tag{3.3}$$

where θ_p is the peak temperature,

$$\alpha^2 = \frac{G'}{(1-\lambda)k} \ , \tag{3.4}$$

and from Eq. (2.10),

$$G' = \frac{\lambda^2}{1-\lambda}\frac{\rho_{cu} j_{\rm op}^2}{\theta_c - \theta_g} \ . \tag{3.5}$$

The boundary of region 2,

$$z_g = \frac{\pi}{2\alpha} \ , \tag{3.6}$$

can be obtained easily from Eq. (3.3). Taking only the conduction term in Eq. (3.1) and using the temperature profile of Eq. (3.3), the equilibrium time τ_c of Eq. (3.2) can be derived readily.

Matching θ and $d\theta/dz$ at $z = z_g$, the solution in region 3 is found to be

$$\theta - \theta_g = -\alpha(\theta_p - \theta_g)(z - z_g) \; . \tag{3.7}$$

The edge of region 3 or the end of the zone is therefore given by

$$z_0 = z_g + \frac{\theta_g - \theta_0}{\alpha(\theta_p - \theta_g)} \; . \tag{3.8}$$

We note that there is a free parameter θ_p in our solution. This is because the continuity of the temperature gradient has not been enforced at $z = z_0$. As a result, there are infinitely many propagating zones. When the peak temperature exceeds θ_c, there are three regions in the propagating zone and therefore 6 constants of integration. By matching the temperature and temperature gradients at $\theta = \theta_c$ and θ_g and also demanding that the temperature gradient should vanish at the center of the heated zone where $z = 0$ (but not at $z = z_0$), only 5 of the constants can be determined. Thus, there are also infinitely many solutions. We try to pick out the solution that contains the minimum energy and define it as the MPZ in our approximation. Figure 7 compares the exact MPZ obtained numerically with the approximate one given by Eqs. (3.3) and (3.7) when $I_{\rm op} = 6.5$ kA. We see that the two temperature profiles agree very well in the generation region ($\theta > \theta_g$). Because they differ when $\theta < \theta_g$, the energy contained in our approximate MPZ is actually smaller.

III.3 Conditions for no solution

In order to obtain the solution for the MPZ, there is a free parameter to vary. It will be nice to know when the solution does not exist so that a possible range of search can be assigned to the parameter.

If the operating current $I_{\rm op}$ is too big so that the NbTi filaments will not be able to carry all the current at bath temperature, or $\theta_g < \theta_0$, heat generation will occur everywhere along the cable. Obviously no stable solution involving finite energy will exist. In fact, no such operation should be designed.

On the other hand, if surface cooling is big enough, no stable heated zone can be established either, because any heat deposited onto the strand will be absorbed completely by the bath at the surface of the strand. Of course, here we imply that the rate at which energy is added should be sufficiently slow so that a steady state can be

reached at any moment and also that the bath temperature θ_0 is always maintained. This criterion can be established mathematically.

We recall that a heated zone with temperature decaying exponentially to the bath temperature in the z-direction requires a maximum amount of energy to set up. Therefore, the strand has zero temperature gradient at the $z_0 = \infty$ end. The temperature gradient at $z = 0$ is also zero. Thus, the equal-area theorem[6] applies (see Appendix for a derivation). The theorem says that this particular stable solution, which corresponds to the maximum energy, exists when the two shaded areas in Fig. 8 are equal. If surface cooling is further increased, no stable solution will exist. In our computation, where the surface cooling of Eq. (2.12) and heat generation of Eqs. (2.10) and (2.11) are assumed, this occurs exactly when

$$\theta_p - \theta_c < \theta_g - \theta_0 \ , \tag{3.9}$$

where θ_p is the peak temperature of the heated zone at $z = 0$, which is determined by the intersection between the cooling and generation curves. Therefore, Eq. (3.2) can be considered as the criterion for safe operation, usually known as cryogenic stability, because no heated zone can be established provided that transient effects can be neglected. However, it should not be mistaken as an operation criterion because a MPZ exists even if the peak temperature θ_p is higher than that given by Eq. (3.2). In fact, a MPZ exists even if there is no surface cooling.

III.4 Method of solution

The steady-state heat flow equation is first solved by assuming that there are only two regions in the heated propagating zone: the region with linear generation when $\theta > \theta_g$ and the region with no generation when $\theta_g > \theta > \theta_0$. By assuming that the thermal conductivity of copper is temperature independent, this temperature profile along the cable can be found easily. The energy stored in this heated zone is next computed according to

$$\mathcal{E} = \int_{-\infty}^{\infty} dz \int_{\theta_0}^{\theta(z)} d\theta \, A C_{\text{eff}}(\theta) \tag{3.10}$$

and then minimized. In Eq. (3.10), C_{eff} is the effective volume specific heat of the strand given by Eq. (2.15), A is the cross-sectional area of the strand, and $\theta(z)$ is the temperature profile of the MPZ. The maximum temperature θ_p is calculated and compared with the critical temperature θ_c. If $\theta_p < \theta_c$, the solution constitutes the MPZ. On the other hand, if $\theta_p > \theta_c$, the computation has not been correct, because the generation should not increase further after θ_c. The computation is then redone by taking into account three regions: $\theta > \theta_c$, $\theta_c > \theta > \theta_g$, and $\theta_g > \theta > \theta_0$. Throughout

the computation, a coil degradation of $D = 5\%$ has been assumed. This implies that the temperature θ_g is derived by equating the critical current density $j_c(\theta_g)$ to $j_{\rm op}/(1-D)$.

IV. RESULTS OF COMPUTATION

IV.1 Energy stored in MPZ

The energy required to set up a MPZ for C358A at bath temperature $\theta_0 = 4.2$ K is shown in Fig. 9(a) as a function of fraction of superconductor in the strand λ. Here, no surface cooling has been assumed and a RRR = 100 for the copper conductivity has been taken. The energy for each operating current exhibits a maximum at some λ. This is expected. The energy required to quench the cable will go to zero when $\lambda \to 1$, because there is not enough the spill-over current and to conduct the heat. It will also go to zero at some small λ corresponding to the critical temperature θ_g, where there will not be enough superconductor to carry the current. For a higher operating current, the temperature θ_g is reached at a higher λ. The energy curve is therefore pushed towards the higher-λ side for larger current. The maximum will be shifted to larger λ. This is evident in Fig. 9(a). For $I_{\rm op} = 7.5$ kA, the maximum energy is 2.79 μJ at $\lambda = 0.76$. If $I_{\rm op}$ is reduced to 5 kA, the maximum energy shoots up to 38.2 μJ at $\lambda = 0.50$, because the point of operation is now much farther away from the thermodynamic surface and more energy will be needed to quench the cable. At $I_{\rm op} = 6.5$ kA, the maximum is 10.41 μJ corresponding to $\lambda = 0.63$. Figure 10 plots the maximum of the energy curve and the λ position for different operating currents. Figure 9(b) shows the same computation as is done in Fig. 9(a) but at $\theta_0 = 4.3$ K. The energy curves are roughly the same, but their values are smaller.

IV.2 Temperature excursion

The temperature excursions, $\theta_p - \theta_0$, of the MPZ's for bath temperatures $\theta_0 = 4.2$ and 4.3 K are shown respectively in Figs. 11(a) and 11(b). Again, RRR = 100 has been assumed and no surface cooling has been included. The peak temperature rises as λ increases. This is due to the fact that there is less copper to carry the spill-over current so that a higher electric field is set up along the cable resulting in more heat generation. Also, heat conduction along the one-dimension cable is less efficient with less copper. The temperature excursion is less than 2.5 K even at $\lambda = 1$.

We see that there is a kink in the 5.0 kA curve, the 5.5 kA curve, and the 6.0 kA curve. The low-λ side of the kink represents MPZ's with only two regions or $\theta_p < \theta_c$. The high-λ side represents MPZ's with three regions or $\theta_p > \theta_c$. For the 6.5 kA,

7.0 kA, and 7.5 kA curves, there are no kinks and they correspond to MPZ's with two regions only. We notice that for the three-region MPZ's, the peak temperature θ_p is nearly independent of λ. In fact, the peak temperature θ_p of a MPZ just barely exceeds the critical temperature θ_c in the central region where NbTi is completely normal.

IV.3 Length of MPZ

The half lengths of the MPZ's are plotted in Figs. 12(a) and 12(b) respectively for $\theta_0 = 4.2$ and 4.3 K as a function of λ. Again, RRR = 100 has been assumed and no surface cooling has been included. The MPZ is set up by the balance between heat generation in the superconductor and heat conduction in the copper. With more copper, therefore, a longer MPZ can be established. As is shown in Fig. 12, the half length of the MPZ is linear with $(1-\lambda)$, the fraction of copper in the strand, and go to zero when there is no copper. The half length is smaller when the bath temperature changes from 4.2 to 4.3 K, but not by very much. However, it does change by very much with the operating current. This is because at lower $I_{\rm op}$, the point of operation is farther away from the thermodynamic surface and more energy can be stored in the MPZ. As a result, the MPZ can spread out over a bigger region resulting in a longer half length. The kinks that separate the two-region MPZ's from the three-region MPZ's are visible for the 5.0 kA, 5.5 kA, and 6.0 kA curves.

The energy of the MPZ per unit length is plotted in Fig. 13. This plot is meaningful because in some cases the MPZ is rather long and of the order of a few mm.

IV.4 Effect of RRR

As is evident from Eqs. (2.10) and (2.11), heat generation is linearly proportional to the resistivity of copper in the cable complex. However, the resistivity of copper arises from two contributions at cryogenic temperatures. As is shown in Eq. (2.13), there is the magneto-resistivity proportional to the magnetic flux density B and the resistivity due to impurities. Although the latter can be reduced by improving copper purity (having a higher RRR), when $B_{\rm max} \sim 7.0$ T the impurity corresponding to RRR = 45 gives roughly the same contribution as the magneto-resistivity. Increasing copper purity, for example to RRR = 100 will decrease copper resistivity by a factor of ~ 0.725. As given by Eq. (3.6), the length of the heated region is inversely proportional to α or $\rho_{cu}^{1/2}$. Thus, the heat content of the MPZ is roughly proportional to $\rho_{cu}^{1/2}$ and is therefore increased by a factor of ~ 1.20. Here, we have assumed that the temperature of the heated zone is not much higher than θ_g and is roughly independent of ρ_{cu}. Note that even if the copper is 100% pure so that RRR = ∞, the heat content of the

MPZ will be increased by only $\sqrt{2}$ compared with RRR = 45 according to our rough estimation.

The energy contained in the MPZ's at operating current $I_{op} = 6.5$ kA and bath temperature $\theta_0 = 4.2$ K without surface cooling is shown in Fig. 14 as a function of fraction of superconductor λ for various values of RRR. Clearly the energy increases with RRR or copper purity, but the increase becomes much slower and the energy tends to a limit when RRR $\gtrsim 50$ as predicted. The dependence on λ is not affected by the value of RRR.

IV.5 Effect of thermal conductivity

As was discussed in the previous section, thermal conductivity of copper k is the main ingredient counteracting heat generation so that a MPZ can be established. The larger k is, the faster an equilibrium can be reached. With a higher efficiency of heat removal, the MPZ can therefore contain more energy. This dependence on k is illustrated in Fig. 15 We see that the fraction of superconductor corresponding to maximum energy remains at $\lambda \sim 0.63$ and does not change with the copper conductivity.

IV.6 Surface cooling

Surface cooling is next introduced and the effect is shown in Fig. 16 at bath temperature $\theta_0 = 4.2$ K, operating current $I_{op} = 6.5$ kA, and RRR = 100. The perimeter-to-area ratio has been taken as $P/A = 2/a$, where a is the radius of one strand. The heat transfer coefficient has been varied from $h = 0$ to 50000 $\mathrm{wm^{-2}K^{-1}}$. We see that the effect of surface cooling is hardly visible when h is less than $\sim$ 1000 $\mathrm{wm^{-2}K^{-1}}$. Even when h rises to 1×10^4 $\mathrm{wm^{-2}K^{-1}}$, the increase in energy contained in the MPZ is still rather small. As was stated in Section II.4, the surface cooling coefficient for one strand in the cable is not known. However, the cable itself is wrapped by a layer of insulation and is not directly in contact with liquid helium. The effective surface heat transfer coefficient is $h = 200$ to 1000 $\mathrm{wm^{-2}K^{-1}}$. Also the ratio P/A is not known. If we take $P/A = 2/\pi a$ instead, the $h = 1000$ $\mathrm{wm^{-2}K^{-1}}$ curve in Fig. 16 corresponds, in fact, to $h = 3142$ $\mathrm{wm^{-2}K^{-1}}$. Thus, for this cable, surface cooling is not an essential effect in determining the minimum energy required to cause a quench, nor in determining the optimized copper-to-superconductor ratio.

The insensitivity of surface cooling can be understood by comparing the cooling effect with heat conduction along the cable making use of the the time-dependent

heat flow equation (3.1). A characteristic surface cooling time of

$$\tau_h = \frac{C_{\rm eff} A}{hP} \cong \frac{C_{\rm eff} a}{2h} \tag{4.1}$$

can be defined, where a is the radius of the strand, $A = \pi a^2$ is the cross sectional area, and $P \sim 2\pi a$ is the perimetric circumference.

We can also define a heat conduction characteristic time for the generation region of the propagating zone, which is just τ_c defined in Eq. (3.2). Taking $z_g = 1.6$ mm (see Table I), $a = 0.404$ mm, $r = 1.3$ ($\lambda = 0.435$), and $k = 350$ w/mK, the ratio of the two characteristic times

$$\frac{\tau_h}{\tau_c} = \frac{\pi^2(1-\lambda)ak}{8hz_g^2} \tag{4.2}$$

is found to be 39, 7.7, and 3.9 when $h = 1000$, 5000, and 10000 $\rm wm^{-2}K^{-1}$. Thus, for $h < 1000$ $\rm wm^{-2}K^{-1}$, it takes at least ~ 39 times longer for heat in the generation region to be transferred through surface cooling than by heat conduction along the cable through the copper when the propagating zone starts propagating.

We notice from Fig. 16 that when h is big enough, the energy curve diverges as λ decreases. This is expected. Decreasing λ implies the introduction of more copper. The smaller fraction of superconductor will increase the operating current density and therefore lower θ_g. The slope of the generation also becomes less steep. Eventually the equal-area criterion of Eq. (3.9) will be met and no stable solution exists. Further decrease in λ will result in the generation slope less than the surface-cooling slope. Therefore, when h is large enough, no solution will exist on the low-λ side. This is just the area discussed in Section III.3 where no solution exists.

V. CONCLUSIONS AND DISCUSSIONS

V.1 Choice of best parameters for cable construction

From our computation results, we can draw some conclusions on the choice of parameters for cable construction.

In order to have a higher energy for the MPZ, we should choose the copper with the lowest electric resistivity ρ_{cu} and the highest thermal conductivity k. However, the lowest ρ_{cu} is dominated by the magneto-resistivity $\rho_{\rm mag}$ which increases linearly with the magnetic flux density B in which the cable is immersed. Economically, it is unwise to choose copper so pure that the RRR is very much larger than $1/\rho_{\rm mag}$. The thermal conductivity is inversely proportional to ρ_{cu} according to Eq. (2.14), and is therefore bounded by the contribution of $\rho_{\rm mag}$.

The superconducting strand will be much more stable for a high surface heat transfer coefficient h. However, for a cable with the conductor not in direct contact with liquid helium, h is usually assumed small and the cooling effect is not noticeable. However, this does not imply that the liquid helium is not important and we can do away with it. Although we find out that the heat in a disturbance or a propagating zone is conducted away along the copper much faster than removed at the surface, the heat conducted away along the copper has to be cooled eventually by the surrounding helium. Also, a surrounding heat bath of a fixed temperature has been assumed throughout the computation. Without the helium circulating at a certain speed, such a bath will not be possible.

The best choice for copper-to-superconductor ratio r is where the energy contained in the MPZ is largest. We see from above that this value of r is not sensitive to variations in the electric resistivity and thermal conductivity of copper. It also does not rely very much on the surface heat transfer coefficient h when h is comparably small. It is also not sensitive to variation of the degradation from 0% to 10%. It only depends on the choice of the operating current $I_{\rm op}$ at a fixed bath temperature. Thus, at $I_{\rm op} = 6.5$ kA, the best choice for copper-to-superconductor ratio appears to be $r = 0.59$ corresponding to $\lambda = 0.63$. Unfortunately, this ratio is far from the 1.3 employed in the C358A Cross Section. However, this is just the *average* ratio. If we examine the cross section of a strand, we find that the NbTi filaments are not distributed uniformly. Instead, we find a copper core of radius ~ 0.085 mm, then an annular band extending out to radius ~ 0.325 mm containing a matrix of NbTi and copper, and finally a copper jacket up a radius 0.404 mm. Inside the annular band, the superconductor filaments are very closely packed. The filaments have a diameter of ~ 5 μm but the spacing between filaments is only ~ 0.5 μm. There is some argument that, the mean-free-path of electrons at cryogenic temperatures is bigger than 0.5 μm, so that the copper in between the filaments may not contribute to thermal conductivity and electrical conductivity. Counting only the interior core and the exterior jacket, the copper-to-superconductor ratio reduces to only 0.91. On the other hand, if we count only the copper in the annular band, the ratio becomes 0.39. Also, there may be some technical reasons that restrict the choice of this ratio. For example, it is impossible to maintain a uniform cross section in fabricating a strand composite with $r < 1$. If the *effective* copper-to-superconductor ratio of C358A is indeed less than 1.3, the thermodynamic phase curve of Eq. (2.4) assumed in our computation will be altered. This will change the critical current density at each temperature and therefore also the temperature θ_g above which power generation begins. It is possible that a different optimum copper content will result.

V.2 Energy of point disturbance required to quench the cable

Our MPZ has a typical half width of $z_0 \sim 3.3$ mm. If the point disturbance has a half width of ~ 3.3 mm, the energy of the MPZ will be the minimum energy of the disturbance required to generate a quench. However, in many cases a point disturbance can have a half width that is very much smaller than ~ 3.3 mm. It will take a finite amount of time, of the order of τ_c, for the disturbance to spread out to the critical temperature profile corresponding to our MPZ. Heat will be generated during this time interval. Therefore, the energy of our MPZ will only be an upper bound of the energy of the original disturbance. We would like to estimate the amount of this heat generated.

Again, let us neglect surface cooling and assume that $\theta < \theta_c$. Integrating the heat flow equation (3.1) along the cable strand, we get for the rate of change of energy $\mathcal{E}$,

$$\frac{d\mathcal{E}}{dt} = G'A \int_{-z_g}^{z_g} dz[\theta(z) - \theta_g] \ . \tag{5.1}$$

Here, no assumption about the profile in the non-generating region is necessary. As a narrow disturbance spreads to the critical temperature profile, the initial rate of drop of the peak temperature θ_p is very fast as is evident from Figs. 5 and 7. For a gaussian initial disturbance, initially $d\theta_p/dt \propto -\theta_p^6$. Most of the time is actually spent in approaching the critical temperature profile. Therefore, Eq. (5.1) can be approximated using Eq. (3.3) as the temperature profile, and we obtain

$$\frac{d\mathcal{E}}{dt} \sim \frac{2AG'(\theta_p - \theta_g)}{\alpha} \ . \tag{5.2}$$

The time spent in approaching the critical profile is of the order

$$\tau_c = \frac{4C_{\rm eff} z_g^2}{\pi^2(1-\lambda)k} \ . \tag{5.3}$$

Therefore, the amount of heat generated in spreading out to the critical temperature profile is of the order

$$\Delta\mathcal{E} \sim \frac{d\mathcal{E}}{dt}\tau_c = \frac{2AC_{\rm eff}(\theta_p - \theta_g)}{\alpha} \ , \tag{5.4}$$

where the relation

$$\alpha^2 = \frac{G'}{(1-\lambda)k} \tag{5.5}$$

has been used. For $I_{\rm op} = 6.5$ kA and copper-to-superconductor ratio 1.3, we get from Table I $\theta_p = 4.889$ K, $\theta_c = 6.107$ K, and $\theta_g = 4.630$ K. We evaluate $C_{\rm eff}$ at θ_p. The

final result is $\Delta\mathcal{E} \sim 1.6\ \mu$J. The computed MPZ has an energy of 6.23 μJ. An actual simulation of the time evolution results in 4.1 μJ for the minimum energy of a narrow disturbance required to start a quench, which is not much different from the difference between 6.23 μJ and 1.6 μJ. But this agreement should not be taken too seriously because our estimation of $\Delta\mathcal{E}$ has been crude. For comparison, we note from Fig. 7 that the *exact* MPZ computed numerically has an energy content of 7.57 μJ, and from Fig. 5 that it takes $\sim 50\ \mu$s for the point disturbance to approach the MPZ. In any case, we can conclude that the energy of our approximate MPZ does give the right order of magnitude for the minimum point energy required to start a quench.

V.3 Contribution of flux jumping

NbTi, being a type II superconductor, can admit magnetic flux. However, the flux penetration is limited by the screening currents which flow with critical current density j_c. As the temperature rises, j_c decreases and more magnetic flux penetrates, thus the energy stored in the superconductor is increased. This effect is known as flux jumping. In this subsection, we are going to show that compared with the minimum energy to start a quench, the energy contribution due to flux jumping is of the same order of magnitude.

For convenience, let us approximate the cylindrical superconductor filament by one having a rectangular cross section $2w \times h$. A coordinate system is set up with the filament running in the y-direction and the side of width $2w$ in the x-direction as shown in Fig. 17. The external magnetic flux density B_{ext} is perpendicular to the filament and is in the z-direction. We assume the critical-state model, which states that all regions of the superconductor are carrying either currents at j_c or no current at all. Thus, there is current of density j_c flowing in the positive y-direction from $x = -w$ to $-w\beta$ and current of density j_c flowing in the negative y-direction from $-w\beta$ to w, so that the net effect is a current of average density

$$j_{\text{op}} = \beta j_c \tag{5.6}$$

flowing in the negative y-direction. The magnetic flux distribution inside the filament is given by Ampere's law

$$\frac{d}{dx}B_{L,R}(x) = \mp\mu_0 j_c\ , \tag{5.7}$$

where L and R denote left and right of the point $x = -w\beta$, and $\mu_0 = 4\pi \times 10^{-7}$ henry/m is the magnetic susceptibility of free space. Integrating Eq. (5.7), we get

$$\begin{cases} B_R(x) &= B_{\text{ext}} + \mu_0 j_c(x - w + w\beta)\ , \\ B_L(x) &= B_{\text{ext}} - \mu_0 j_c(x + w + w\beta)\ . \end{cases} \tag{5.8}$$

The constants of integration have been so chosen that

$$\begin{cases} B_R(-w) + B_L(w) = 2B_{\text{ext}} \ , \\ B_R(-w\beta) = B_L(-w\beta) \ . \end{cases} \tag{5.9}$$

The energy of the magnetic flux for a length ℓ of the filament at operation is

$$\mathcal{E}_{\text{op}} = \frac{h\ell}{2\mu_0} \left[\int_{-w}^{-w\beta} B_L^2(x)dx + \int_{-w\beta}^{w} B_R^2(x)dx \right] \ . \tag{5.10}$$

When the superconductor becomes normal, we assume that all the current is displaced to the copper and the external magnetic flux penetrates completely. The magnetic energy becomes

$$\mathcal{E}_{\text{norm}} = \frac{h\ell}{2\mu_o} \left[2wB_{\text{ext}}^2 \right] \ . \tag{5.11}$$

The increase in energy due to flux jumping is therefore

$$\Delta\mathcal{E} = \mathcal{E}_{\text{norm}} - \mathcal{E}_{\text{op}} \ . \tag{5.12}$$

With the help of Eqs. (5.8) to (5.11), we get

$$\Delta\mathcal{E} = h\ell j_c w^2 \left[B_{\text{ext}}(1-\beta^2) - \frac{1}{3}\mu_0 j_c w \right] \ , \tag{5.13}$$

where the second term in the square brackets is small and can be neglected. At $B_{\text{ext}} = 6.6$ T, $j_c = 1.62 \times 10^9$ A/m^2 with 5% degradation. With $j_{\text{op}} = 1.27 \times 10^9$ A/m^2, $\beta = 0.78$. We also assume $w = 2.5$ μm, the radius of the filament. This leads to $\Delta\mathcal{E} = 0.026h\ell$ J. For a whole strand composite, we multiply by $\lambda A/2wh$, where $\lambda = 1/2.3$ is the fraction of superconductor and $A = 5.13 \times 10^{-7}$ m^2 is the cross sectional area of the strand. Then, the energy contribution of flux jumping becomes $\Delta\mathcal{E} = 1.2$ μJ/mm. Thus, the effect of flux jumping is of the same order as the heat content of the MPZ. This effect should be included in a more complete analysis.

V.4 Linearity of heat generation

The heat generation per unit volume given by Eq. (2.10) is linear with the temperature θ. In this section, we would like to investigate the validity of this expression.

Three assumptions have been made in deriving Eq. (2.10). First, we assume that the temperature distribution in the strand is uniform transversely. This is true for the copper but not the NbTi filaments, because NbTi is a poor thermal conductor. If

the temperature does not change too rapidly during a heat generation, we can write a steady-state local heat balance equation[8]

$$-k_{sc}\frac{1}{r}\left(r\frac{d\theta}{dr}\right) = Ej_c(\theta) = Ej_c(\theta_n)\frac{\theta_c-\theta}{\theta_c-\theta_n}\ , \tag{5.14}$$

where r is the radial distance from the center of a NbTi filament, k_{sc} is the conductivity of NbTi, θ_n is the temperature of the surrounding copper, E is the electric field set up by the spill-over current and is given by Eq. (2.7) with j_c replaced by j_{cav}, the average current density across the filament. The radial temperature profile can be easily found to be

$$\theta(r) = \theta_n + (\theta_c-\theta_n)\left[1-\frac{I_0(\alpha r/r_0)}{I_0(\alpha)}\right]\ , \tag{5.15}$$

where r_0 the radius of the NbTi filament and

$$\left(\frac{\alpha}{r_0}\right)^2 = \frac{Ej_c(\theta_n)}{k_{sc}(\theta_c-\theta_n)}\ . \tag{5.16}$$

The mean current density over the filament can then be computed,

$$j_{cav} = j_c(\theta_n)\frac{2I_1(\alpha)}{\alpha I_0(\alpha)}\ , \tag{5.17}$$

where I_0 and I_1 are modified Bessel functions of the first kind. Using Eqs. (2.8), (2.9), and (5.17), the power generation of Eq. (2.10) is now modified to

$$\frac{G(\theta_n)}{G_c} = 1-\left[\frac{\theta_c-\theta_n}{\theta_c-\theta_g}\right]\left[\frac{2I_1(\alpha)}{\alpha I_0(\alpha)}\right]\ . \tag{5.18}$$

Since α depends on θ_n, the generation in Eq. (5.18) is no longer linear. Next we wish to solve for α and determine the nonlinearity. We define a characteristic length

$$d^2 = \frac{k_{sc}(1-\lambda)(\theta_c-\theta_g)}{\lambda\rho_{cu}j_{\rm op}^2}\ , \tag{5.19}$$

in terms of which, α in Eq. (5.16) can be rewritten as

$$\alpha^2 = \frac{r_0^2}{d^2}\frac{G(\theta_n)}{G_c}\ . \tag{5.20}$$

Now the generation can be obtained from Eqs. (5.18) and (5.20) by eliminating α. The result is shown in Fig. 18 for various values of $(r_0/d)^2$. For the C358A cable, there are $N = 11000$ filaments in a strand corresponding to a filament radius of $r_0 \sim 0.25$ μm.

If we take $k_{sc} = 0.1$ w/mK, $\rho_{cu} = 3 \times 10^{-10}$ Ωm, copper-to-superconductor ratio = 1.3, and operating current $I_{\rm op} = 6.5$ kA, we get

$$\frac{r_0^2}{d^2} = \frac{0.025}{\theta_c - \theta_g} , \tag{5.21}$$

or 0.017 with $\theta_c - \theta_g = 1.48$ K from our computation. Thus, according to Fig. 18, the effect of nonuniform transverse temperature across the NbTi filaments to the nonlinearity of the generation curve is minimal.

Second, the thermodynamic curve that separates the superconducting phase and normal phase of NbTi at a fixed magnetic flux density has been assumed to be a straight line. We can see from Fig. 2 that this thermodynamic curve is almost but not exactly straight. In our computation, we draw a tangent to the thermodynamic curve at the point ($j_{\rm op}$, θ_g) and call θ_c the point of intersection between the tangent and the θ-axis. Our general results in Table I show that there is only a small variation in θ_c for different copper-to-superconductor ratios for each fixed operating current $I_{\rm op}$ or fixed maximum magnetic flux density $B_{\rm max}$. The straight line assumption of the thermodynamic curve appears to be quite good.

Third, the resistivity of cable as a whole is assumed to follow $(j_{\rm op}/j_c)^n$ with $n = \infty$ when $j_{\rm op} > j_c$. In fact, experimental measurement reveals that $n \sim 20$ to 30. The absence of a sharp critical current density is believed due to the nonuniformity of the superconductor filaments inside the cable. In other words, each filament may have a slightly different critical current density at a given temperature and magnetic flux density. As a result, the generation curve will start to rise from θ_g with a high-power dependence on temperature. Effectively, this phenomenon increases j_c, θ_g, and θ_c, if we continue to assume an approximate linear generation curve. The minimum energy to start a quench can be increased[9] by $\sim$50%. The optimum copper-to-superconductor ratio may also be affected.

ACKNOWLEGEMENTS

The author wishes to thank Drs. A. Tollestrup and S. Wipf for interesting and stimulating discussions on the subject of MPZ. He is extremely grateful to many valuable discussions with Dr. R. Stiening. He also wishes to acknowledge Dr. A. Chao for encouragement and helpful discussions while this work was done.

APPENDIX

The one-dimension heat flow equation, Eq. (3.1) with the time-dependent term deleted, can be solved exactly if we transform it into

$$\frac{dS^2}{d\theta} = 2k(\theta)\left[\frac{PH(\theta)}{A} - G(\theta)\right] \tag{A.1}$$

by defining

$$S(\theta) = k(\theta)\frac{d\theta}{dz} , \tag{A.2}$$

so that

$$\frac{dS}{dz} = \frac{dS}{d\theta}\frac{d\theta}{dz} = \frac{1}{2k}\frac{dS^2}{d\theta} . \tag{A.3}$$

Consider a one dimension rod with temperature θ_0 at one end and temperature θ_p at the other end. If the temperature gradients are zero at both ends, then the integration of Eq. (A.1) gives

$$\int_{\theta_0}^{\theta_p} k(\theta)\left[\frac{PH(\theta)}{A} - G(\theta)\right] = 0 , \tag{A.4}$$

implying equal area under the cooling and heat generation curves when multiplied by $k(\theta)$. Note that if θ_0 is the bath temperature, usually $PH = GA$ there because PH and GA vanish separately. However, PH need not equal GA at the high-temperature end, because, in general, the divergence of the temperature gradient does not vanish there, when surface cooling is present. Therefore, θ_p need not be the intersection of the heating and cooling curves, and the equal-area theorem can imply something like Fig. 19. The equal-area theorem fails when the zone is of finite length. This is because the temperature gradient at the end of the zone will not vanish and is balanced by heat conduction instead. Thus, the equal-area theorem, although simple, does not really provide us with a stability criterion for the SSC dipole cable.

REFERENCES

1. S.L. Wipf, Los Alamos Scientific Laboratory Report, LA7275, 1978.

2. M.N. Wilson, *Superconducting Magnets*, Clarendon, 1983. The computation of MPZ is illustrated there in one and three dimensions. However, the computation has been limited to only two heated regions and has not been extended to include surface cooling. Most of the materials in our computation are taken from this reference.

3. K.Y. Ng, SSC Report SSC-N-521, 1988. There is an error in the effective heat capacity of the strand composite in this preliminary report.

4. P. Wanderer, addendum to Ref. 5.

5. G. Morgan, SSC Magnet Division Note No. 110-4 (SSC-MD-84), 1984.

6. see for example, R.E. Peierls, *Quantum Theory of Solids,* Oxford, Clarendon Press, p.121.

7. B.J. Maddock, G.B. James, and W.T. Norris, Cryogenics Aug., 261 (1969).

8. This discussion is taken from Ref 2.

9. S.L. Wipf, Private communication.

VOLUME HEAT CAPACITY OF CU = 1.600E+03 J/M^3.K
VOLUME HEAT CAPACITY OF SC = 6.800E+03 J/M^3.K
HEAT CONDUCTIVITY OF SC = 350.0 W/M.K
HEAT TRANSFER COEFF = 1.000E-02 W/M^2.K
AREA OF 1 STRAND OF CABLE = 5.128E-07 M^2

BATH TEMPERATURE = 4.20 K
DEGRADATION = 95.0 %

T_G IS TEMP ON CRITICAL THERMODYNAMIC SURFACE CORR TO OPERATING CURRENT I_OP AND CU TO SUPER COND RATIO R. THE RESULTING CENTRAL MAGNETIC FIELD IS B. Z_0 IS HALF-WIDTH OF MPZ AND Z_G IS HALF WIDTH OF THE PART WITH GENERATION. AN * AT THE RIGHT INDICATES THAT THE PEAK TEMP T_P OF MPZ EXCEEDS THE CRITICAL LIMITING TEMP T_C; THE ENERGY E TO START A QUENCH IS THEN AN OVERESTIMATE.

I_OP (KA)	B (T)	R CU/SC	T_G (K)	T_C (K)	T_P (K)	Z_0 (MM)	Z_G (MM)	Z_C (MM)	E (MICRO J)	
6.500	6.6015	0.50	5.1352	6.0710	5.6251	1.6557	0.7474	0.0000	1.0264D+01	
6.500	6.6015	0.60	5.0727	6.0731	5.5370	1.9098	0.8694	0.0000	1.0405D+01	
6.500	6.6015	0.70	5.0101	6.0758	5.4480	2.1458	0.9853	0.0000	1.0255D+01	
6.500	6.6015	0.80	4.9474	6.0790	5.3580	2.3657	1.0959	0.0000	9.8858D+00	
6.500	6.6015	0.90	4.8844	6.0830	5.2669	2.5713	1.2021	0.0000	9.3505D+00	
6.500	6.6015	1.00	4.8212	6.0877	5.1746	2.7639	1.3043	0.0000	8.6896D+00	
6.500	6.6015	1.10	4.7577	6.0932	5.0809	2.9446	1.4031	0.0000	7.9340D+00	
6.500	6.6015	1.20	4.6940	6.0995	4.9858	3.1144	1.4989	0.0000	7.1077D+00	
6.500	6.6015	1.30	4.6300	6.1069	4.8891	3.2741	1.5922	0.0000	6.2295D+00	
6.500	6.6015	1.40	4.5656	6.1154	4.7906	3.4245	1.6833	0.0000	5.3144D+00	
6.500	6.6015	1.50	4.5008	6.1250	4.6900	3.5660	1.7724	0.0000	4.3742D+00	
6.500	6.6015	1.60	4.4356	6.1359	4.5873	3.6990	1.8600	0.0000	3.4186D+00	
6.500	6.6015	1.70	4.3700	6.1482	4.4822	3.8241	1.9462	0.0000	2.4553D+00	
6.500	6.6015	1.80	4.3039	6.1621	4.3742	3.9413	2.0313	0.0000	1.4907D+00	
RESISTIVITY OF CU = 5.291E-10 OHM.M, RRR = 100.0										
5.000	5.1675	0.50	6.0197	6.6809	6.6809	2.4344	0.8845	0.0015	3.3208D+01	*
5.000	5.1675	0.60	5.9757	6.6793	6.6793	2.6758	1.0266	0.0016	3.5185D+01	*
5.000	5.1675	0.70	5.9318	6.6778	6.6778	2.8759	1.1607	0.0017	3.6568D+01	*
5.000	5.1675	0.80	5.8879	6.6764	6.6451	3.1158	1.2879	0.0000	3.7503D+01	
5.000	5.1675	0.90	5.8442	6.6750	6.5874	3.3934	1.4091	0.0000	3.8013D+01	
5.000	5.1675	1.00	5.8005	6.6737	6.5297	3.6553	1.5249	0.0000	3.8175D+01	
5.000	5.1675	1.10	5.7568	6.6726	6.4719	3.9031	1.6358	0.0000	3.8057D+01	
5.000	5.1675	1.20	5.7132	6.6715	6.4140	4.1381	1.7425	0.0000	3.7713D+01	
5.000	5.1675	1.30	5.6697	6.6706	6.3560	4.3614	1.8454	0.0000	3.7187D+01	
5.000	5.1675	1.40	5.6262	6.6698	6.2978	4.5741	1.9448	0.0000	3.6513D+01	
5.000	5.1675	1.50	5.5827	6.6692	6.2394	4.7769	2.0410	0.0000	3.5717D+01	
5.000	5.1675	1.60	5.5393	6.6688	6.1809	4.9706	2.1344	0.0000	3.4824D+01	
5.000	5.1675	1.70	5.4959	6.6685	6.1222	5.1559	2.2252	0.0000	3.3850D+01	
5.000	5.1675	1.80	5.4524	6.6685	6.0633	5.3334	2.3136	0.0000	3.2811D+01	
RESISTIVITY OF CU = 4.511E-10 OHM.M, RRR = 100.0										

Table 1

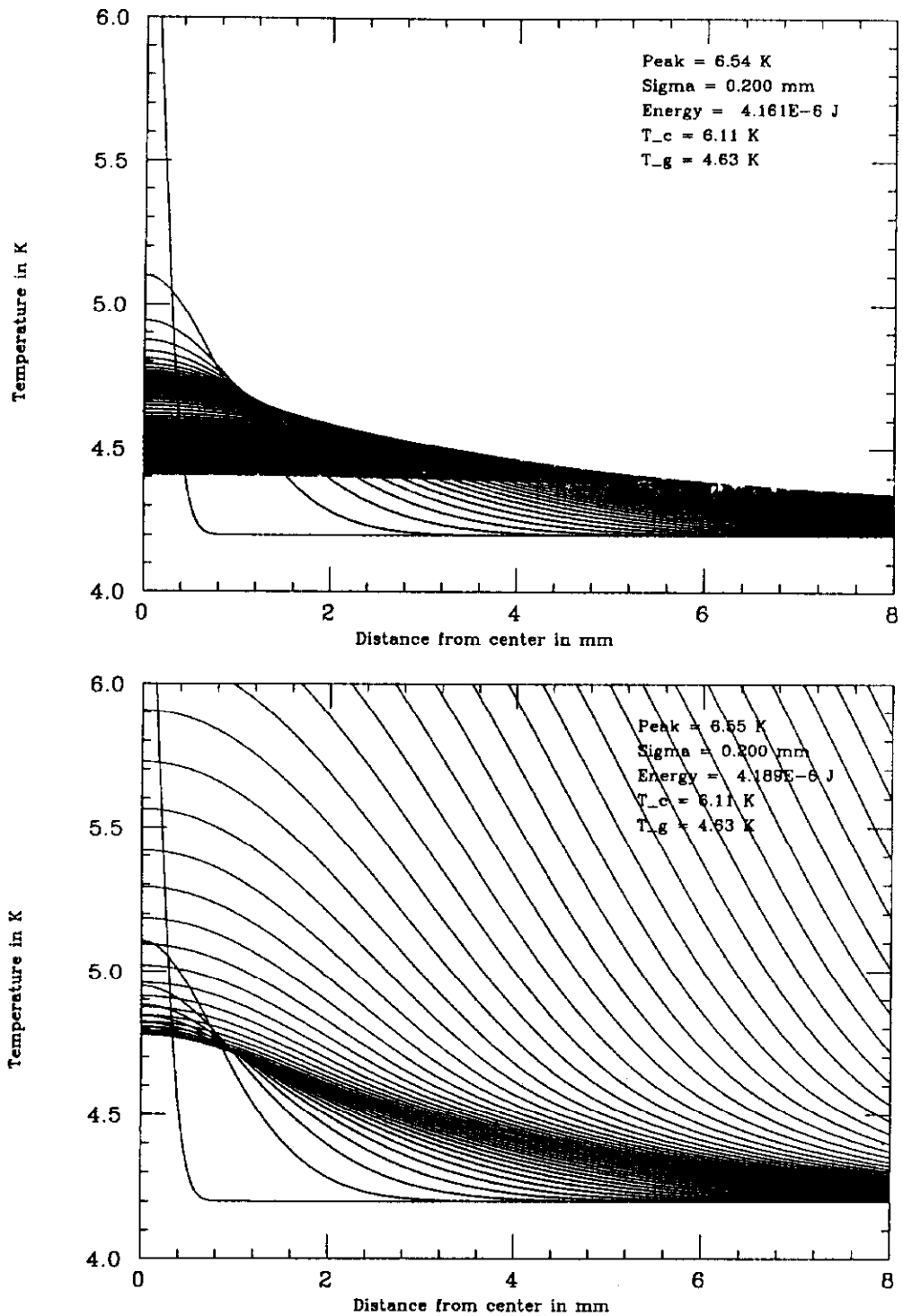

Fig. 1. Time evolution of a gaussian point disturbance. The disturbance spreads out initially and then approaches a critical temperature profile slowly. After that (a) the critical temperature profile subsides if the initial energy deposition is small. (b) The critical temperature profile diverges if the initial energy deposition is big.

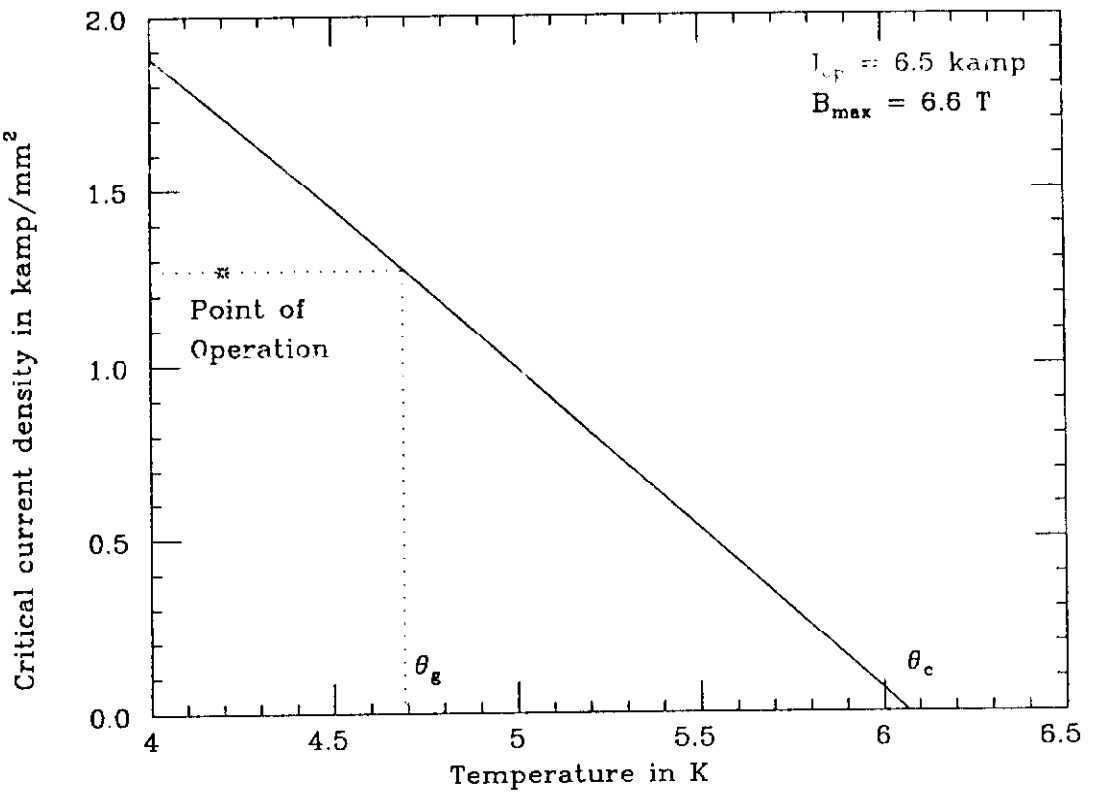

Fig. 2. Thermodynamic curve separating the superconducting phase from the normal phase. No degradation is assumed.

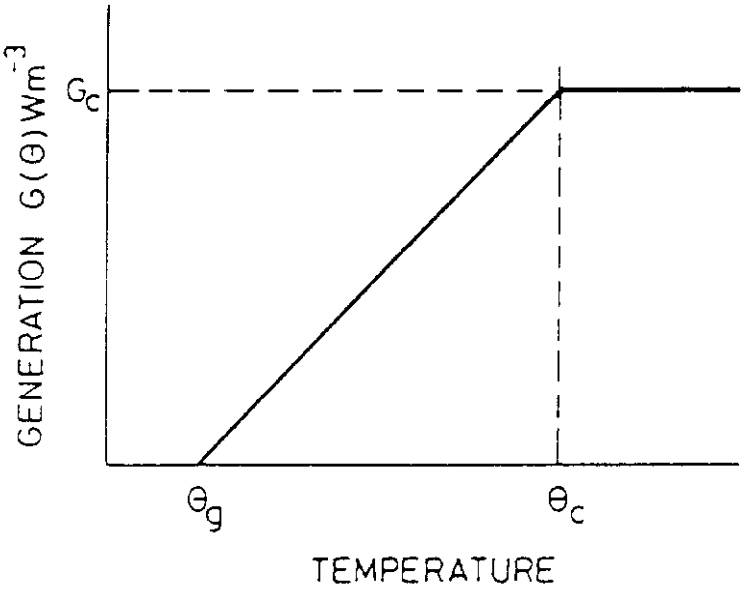

Fig. 3. Temperature dependence of power generation in a composite superconductor strand.

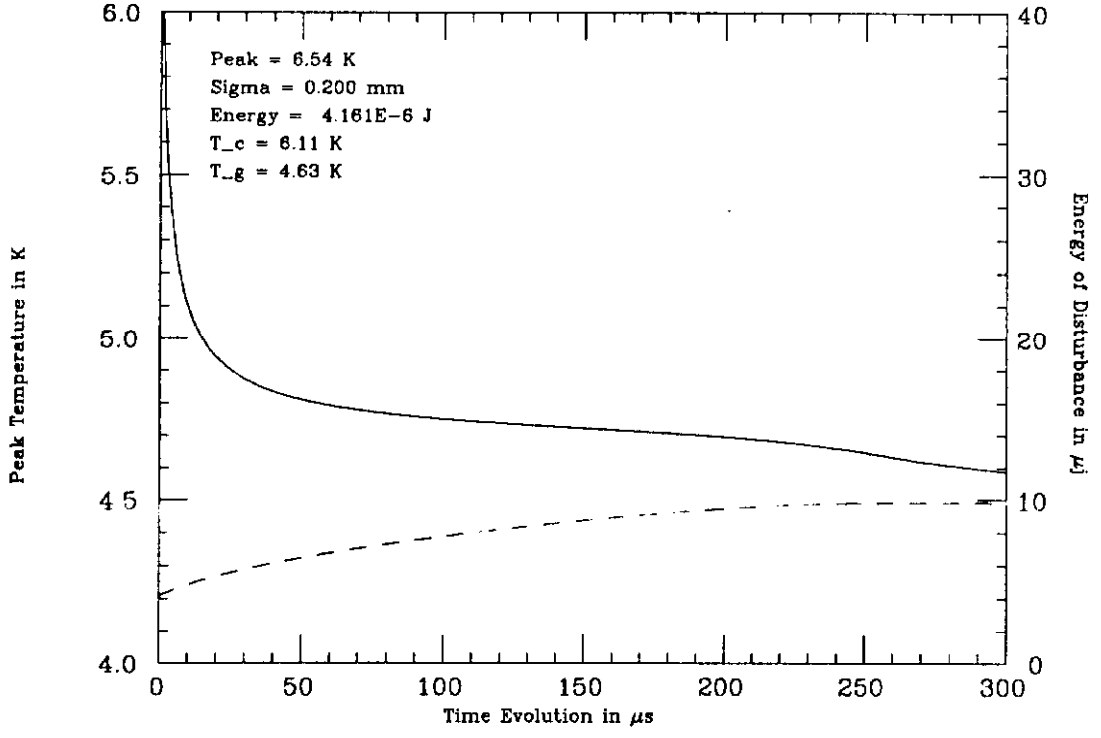

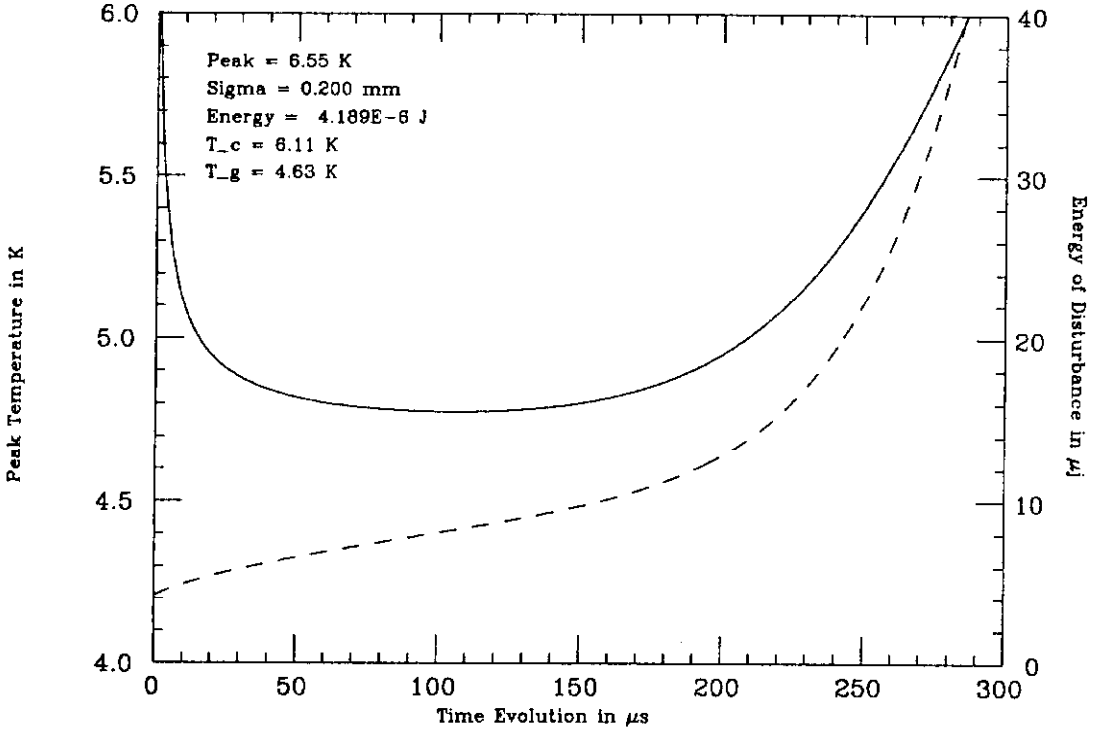

Fig. 4. Time evolutions of peak temperature and energy for a point disturbance. The subsiding of the disturbance in (a) corresponds to the temperature profiles shown in Fig. 1(a). The divergence of the disturbance in (b) corresponds to the temperature profiles shown in Fig. 1(b).

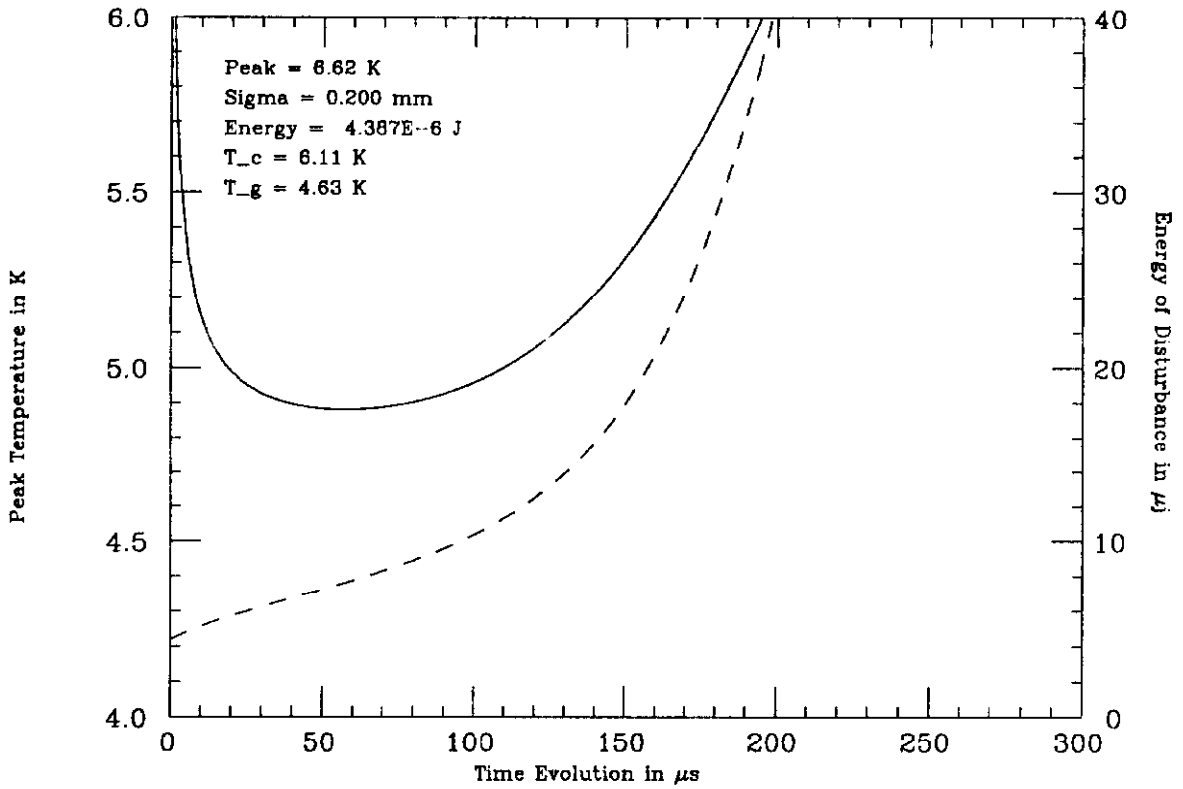

Fig. 5. Time evolutions of peak temperature and energy of the point disturbance that develops into the MPZ.

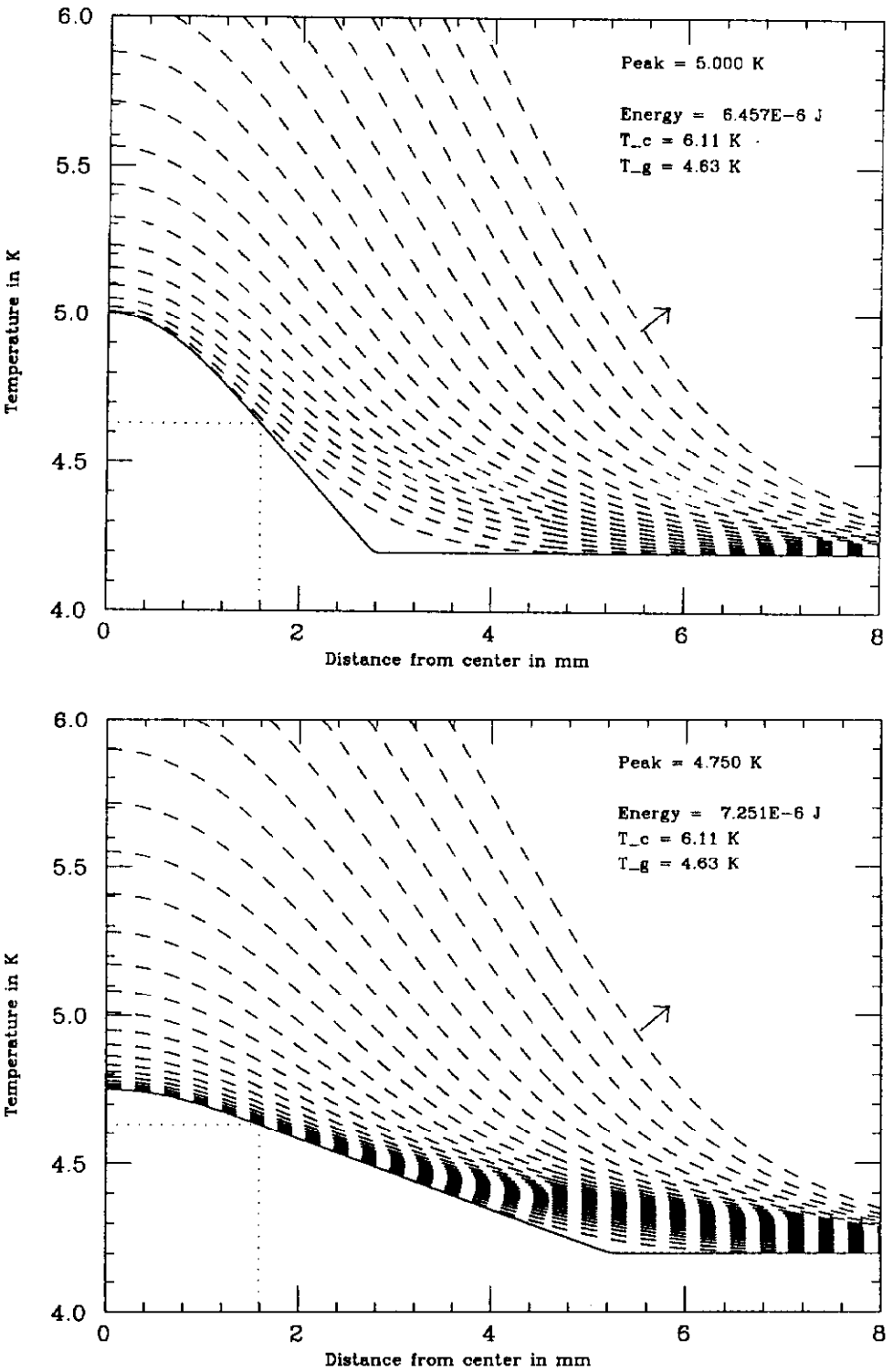

Fig. 6. Two approximate propagating zones (solid curves) and their future time evolutions.

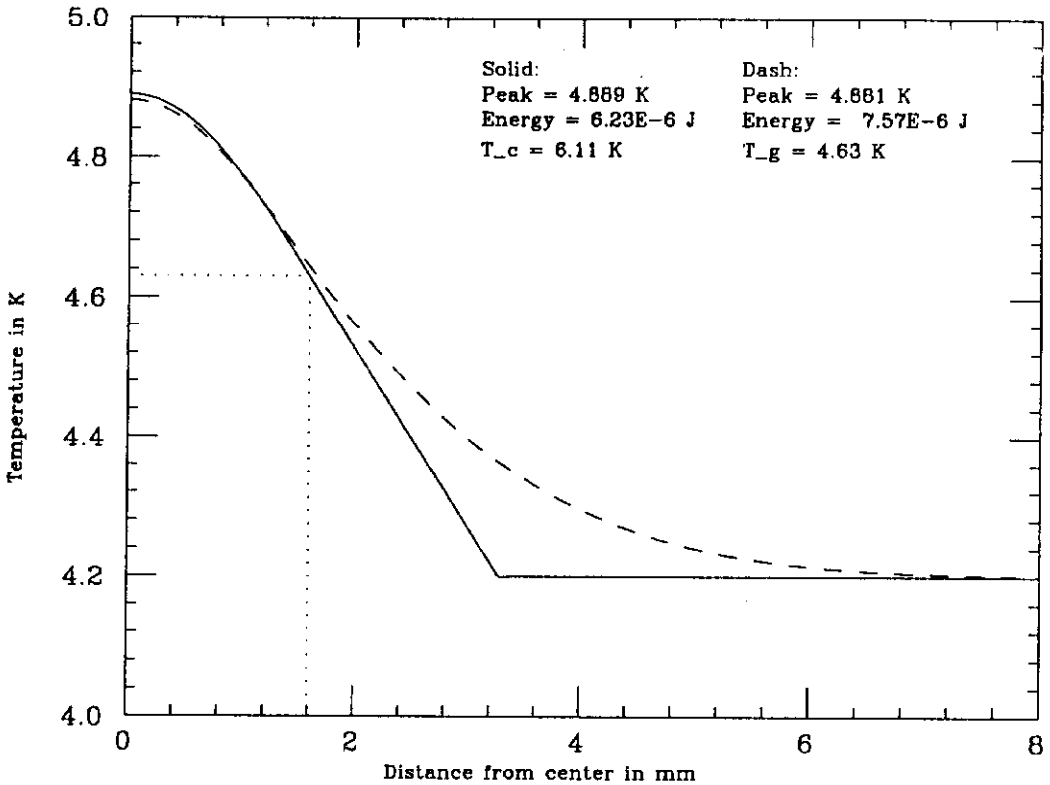

Fig. 7. Comparison of the *exact* numerically computed MPZ (dashes) and our approximate MPZ (solid).

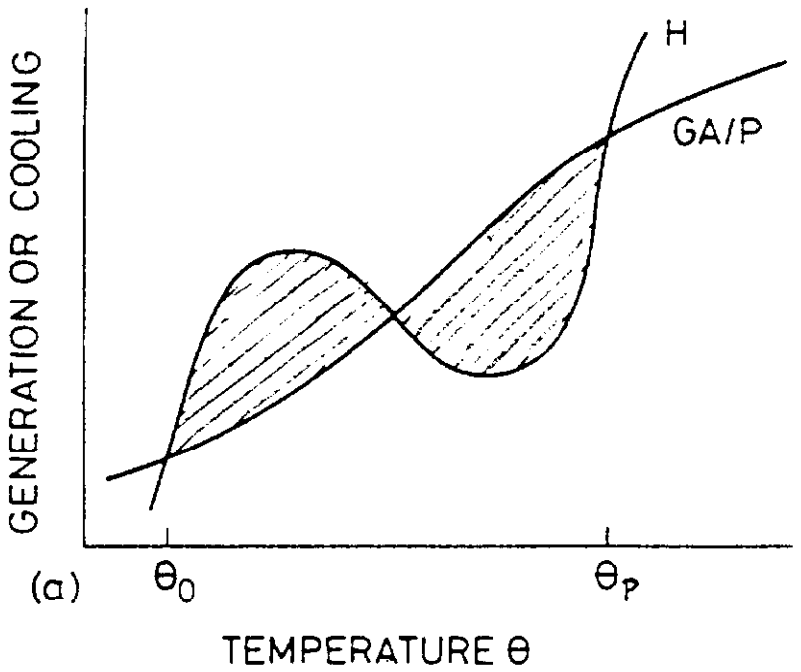

Fig. 8. A stable solution implied by the equal-area theorem. Note that the two shaded areas are equal.

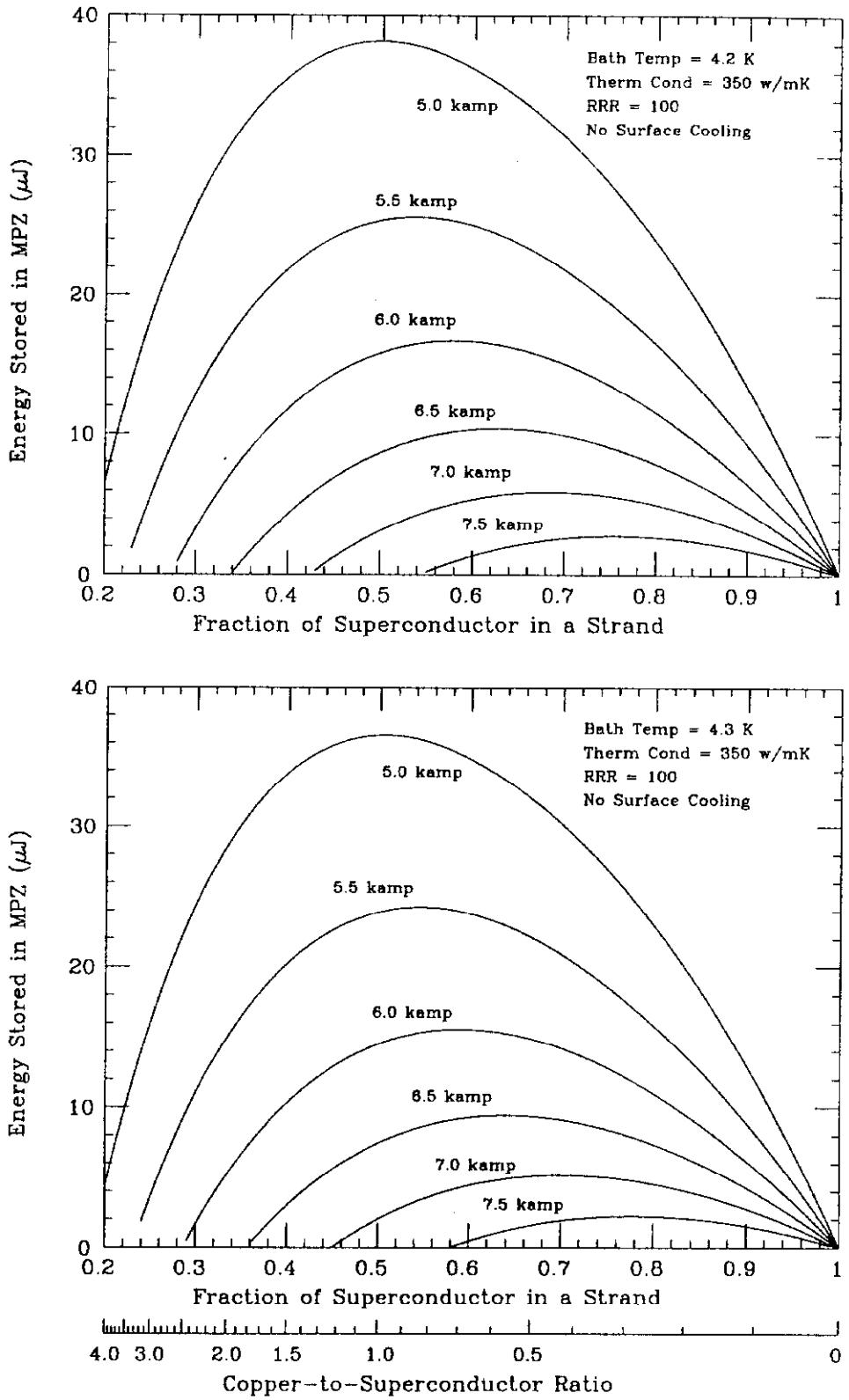

Fig. 9. Energy stored in MPZ with bath temperature (a) 4.2 K and (b) 4.3 K. A 5% degradation has been assumed.

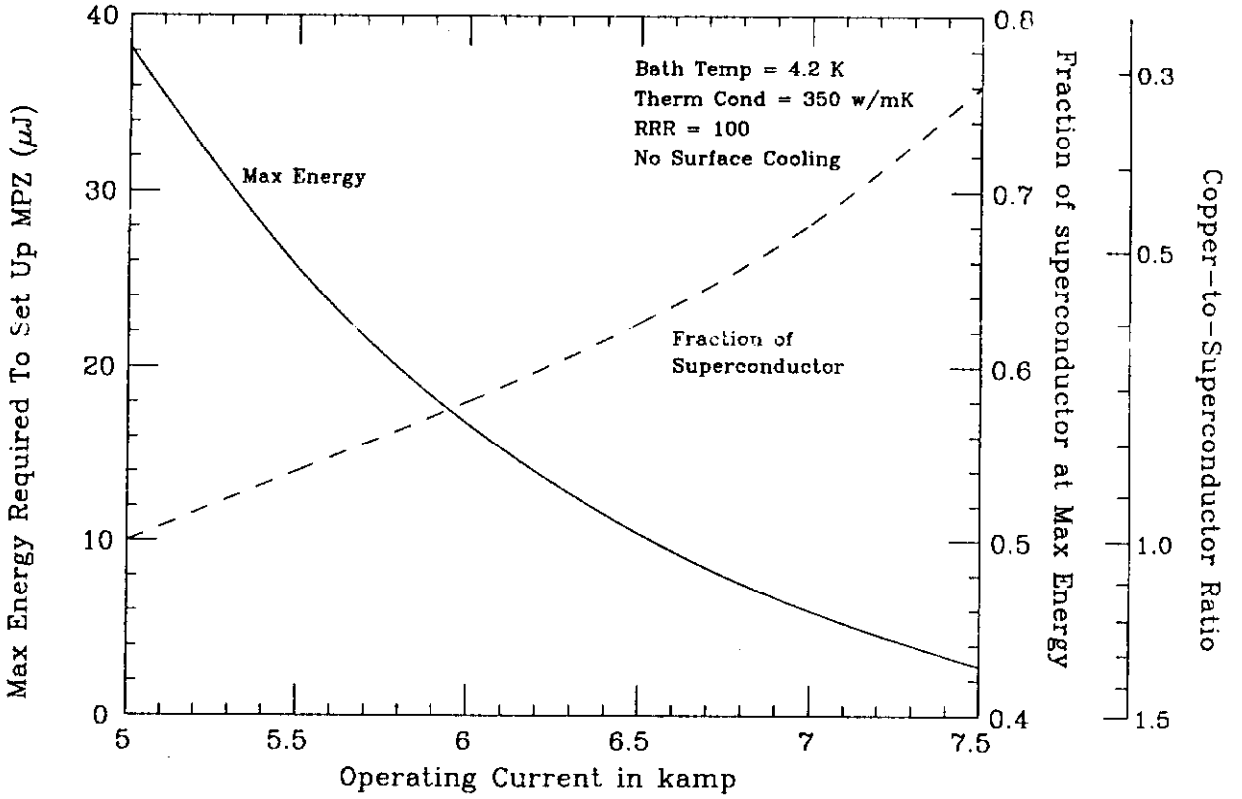

Fig. 10. Plots of maximum energy in the MPZ and position of maximum verses operating current. A 5% degradation has been assumed.

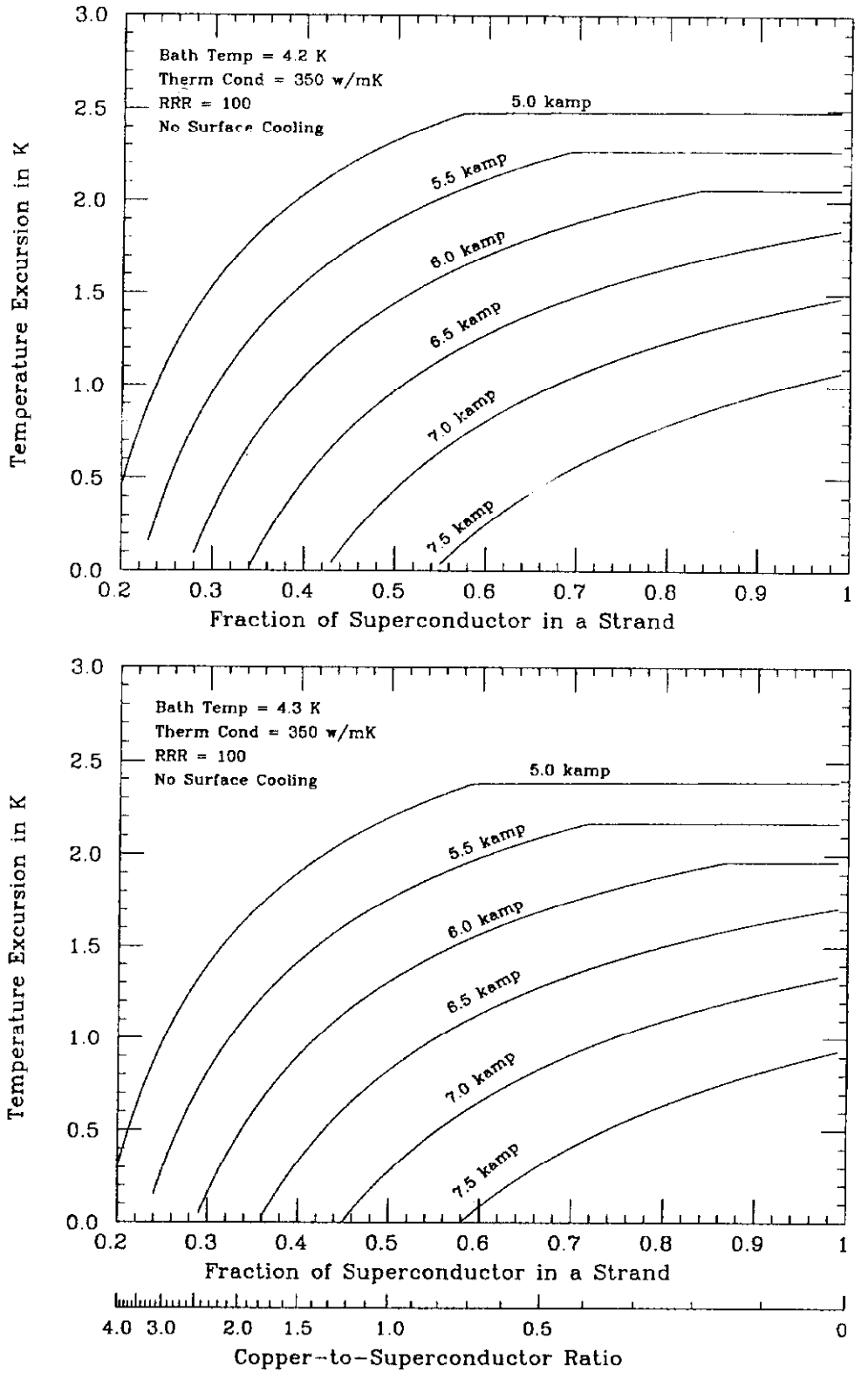

Fig. 11. Temperature excursion in the MPZ with bath temperature (a) 4.2 K and (b) 4.3 K. A 5% degradation has been assumed.

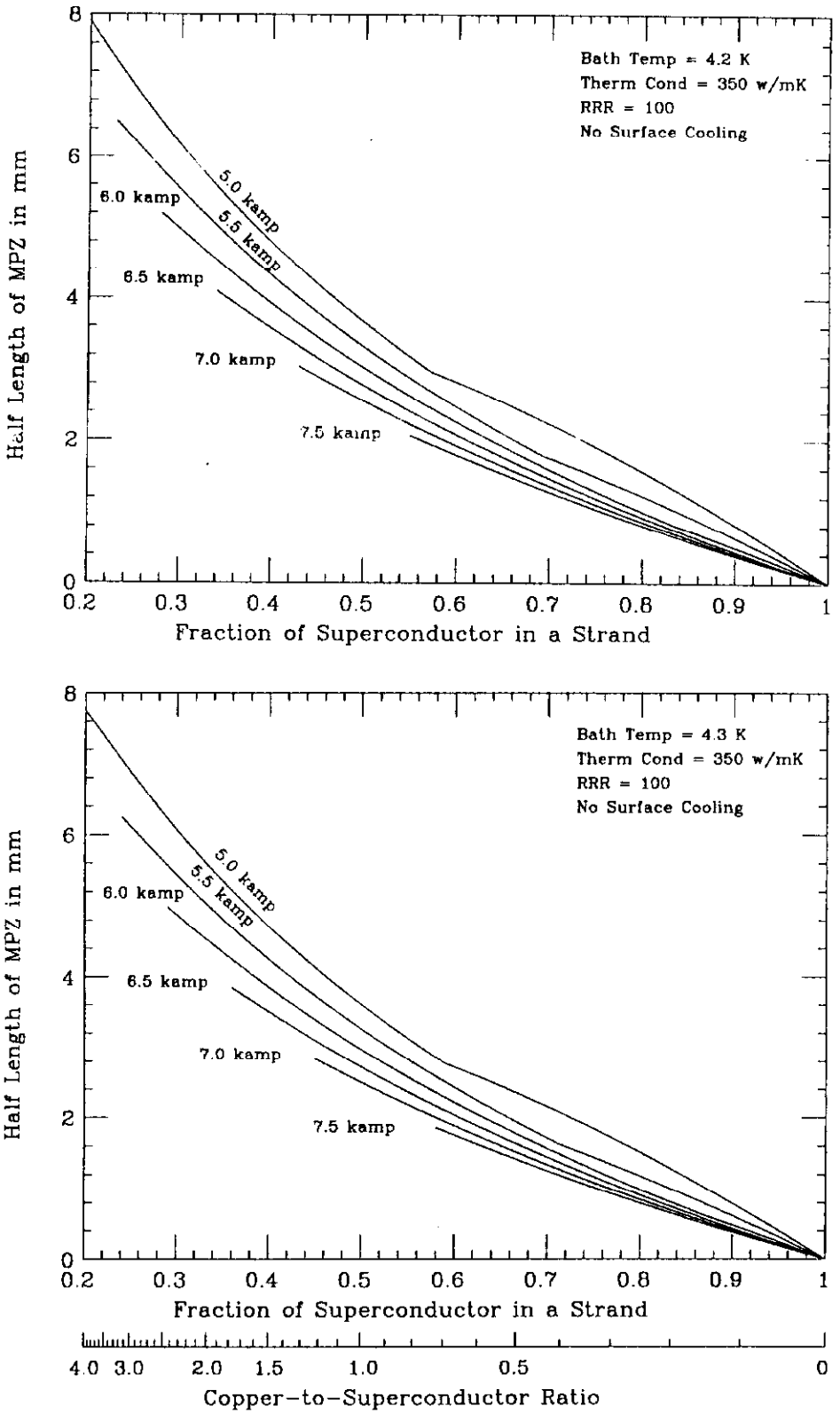

Fig. 12. Half length of the MPZ up to where the temperature equals bath temperature. A 5% degradation has been assumed.

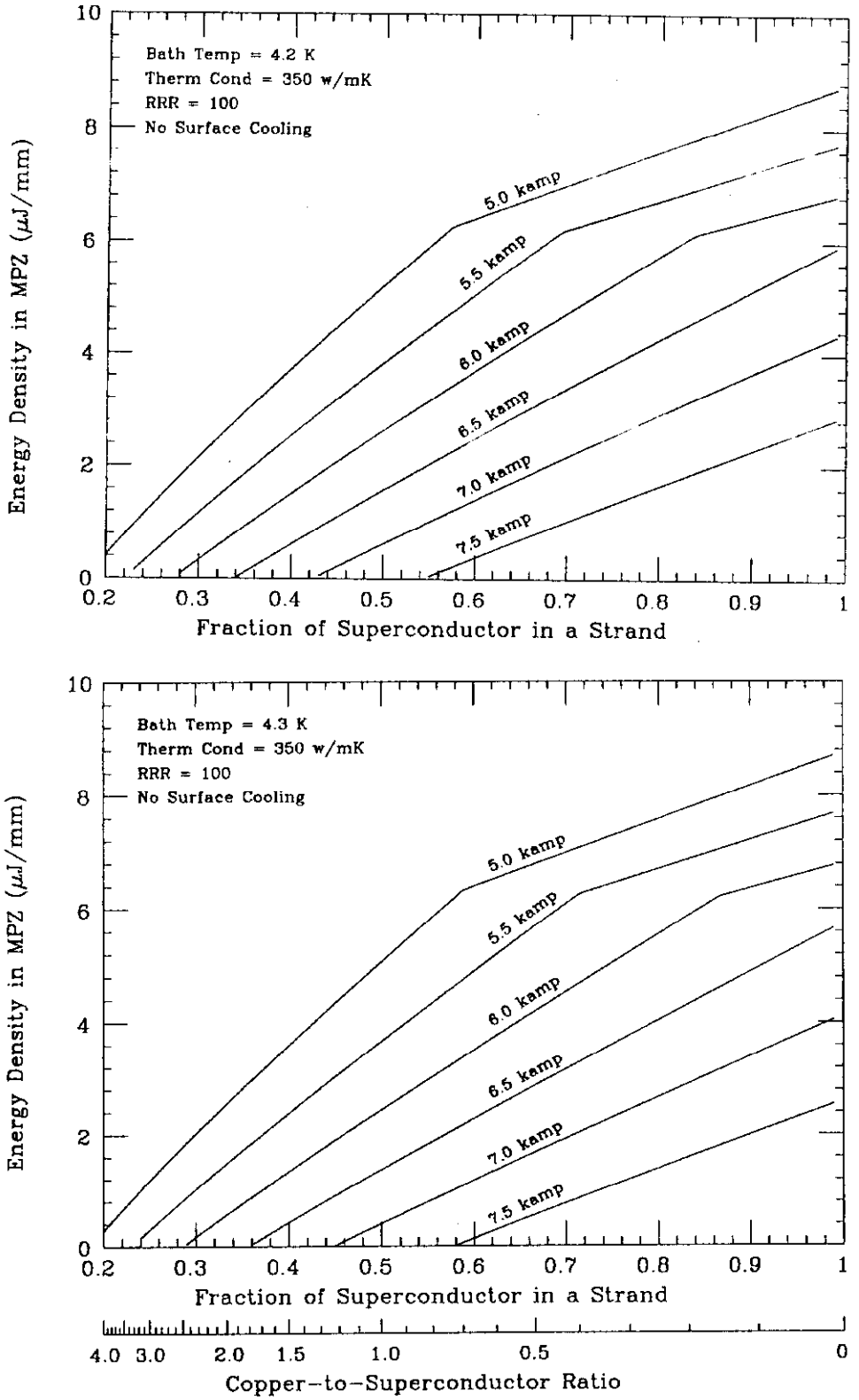

Fig. 13. Energy stored in the MPZ per unit length. A 5% degradation has been assumed.

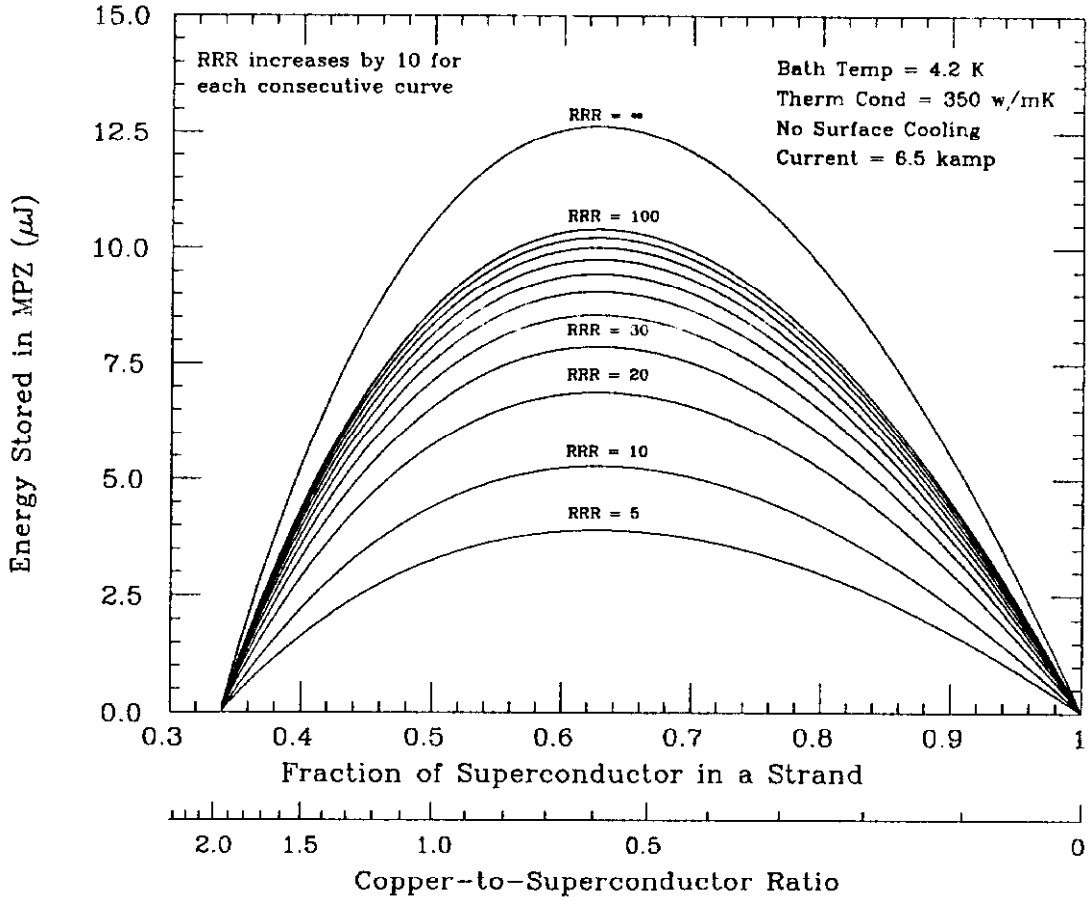

Fig. 14. Variation of MPZ's energy with RRR of copper. A 5% degradation has been assumed.

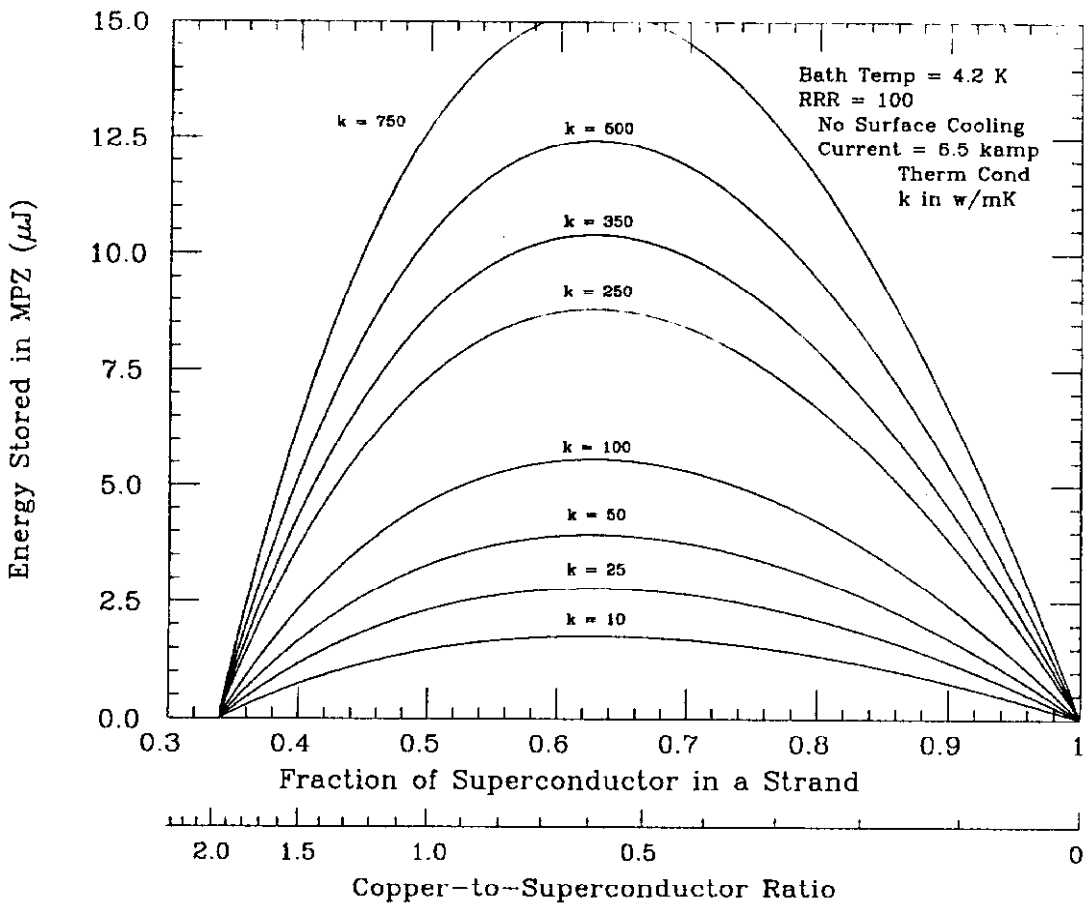

Fig. 15. Variation of MPZ's energy with thermal conductivity of copper. A 5% degradation has been assumed.

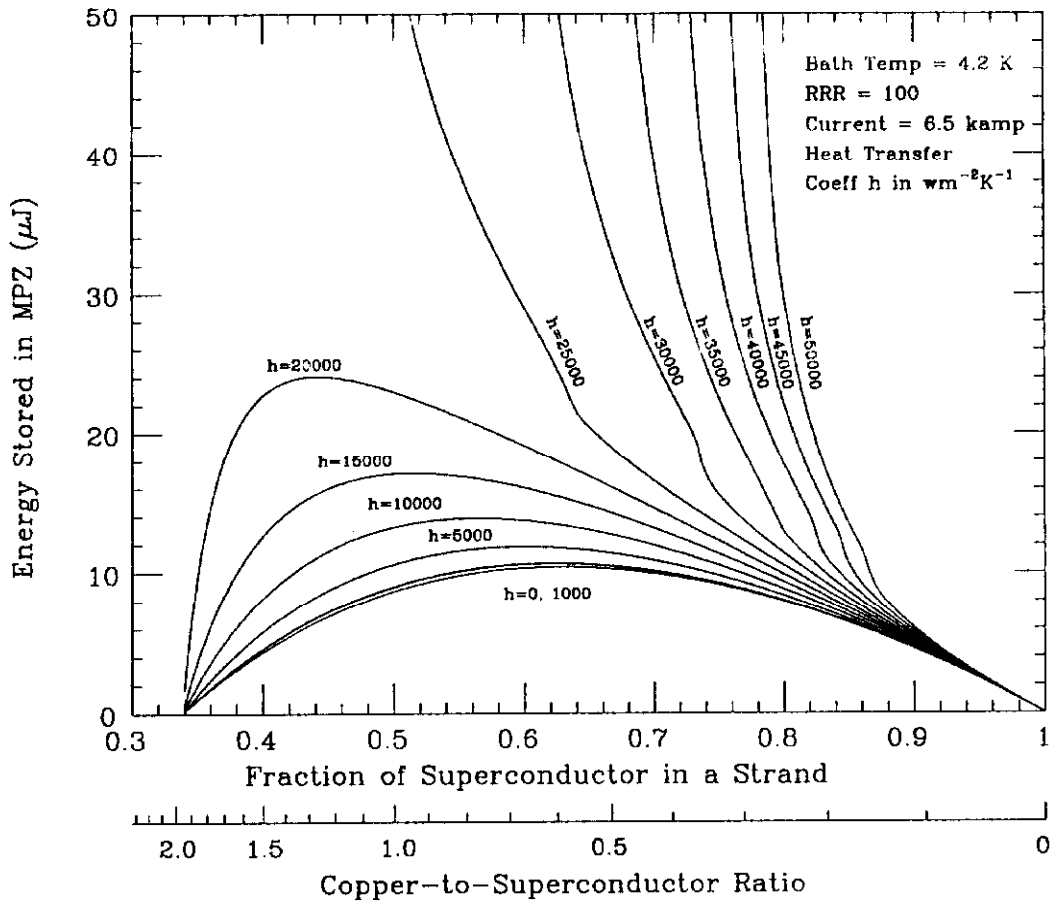

Fig. 16. The effect of surface cooling with a 5% degradation assumed. The perimeter-to-area ratio has been taken as that for a cylinder, or $P/A = 2/a$, where a is the radius of one strand. The curves for different values of P/A can be obtained by scaling h. It is possible that $P/A \sim 2/\pi a$ if the whole cable is considered. If only the narrow edges of the cable are cooled, $P/A \sim 8/S\pi a$, where $S = 23$ is the number of strands in the cable.

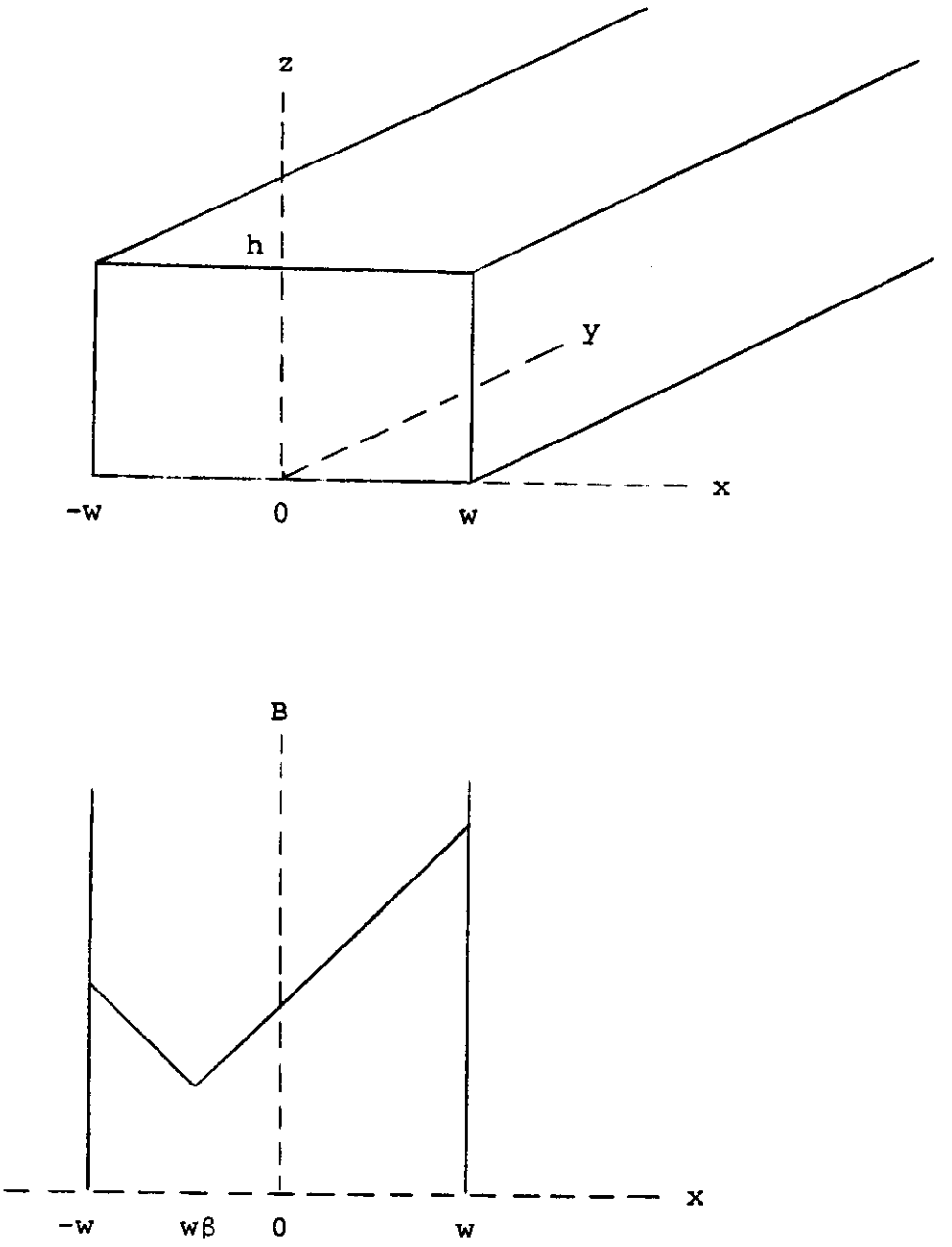

Fig. 17. (a) A superconductor filament with approximate rectangular cross section in a magnetic field B_{ext}. (b) Magnetic field pattern across the filament.

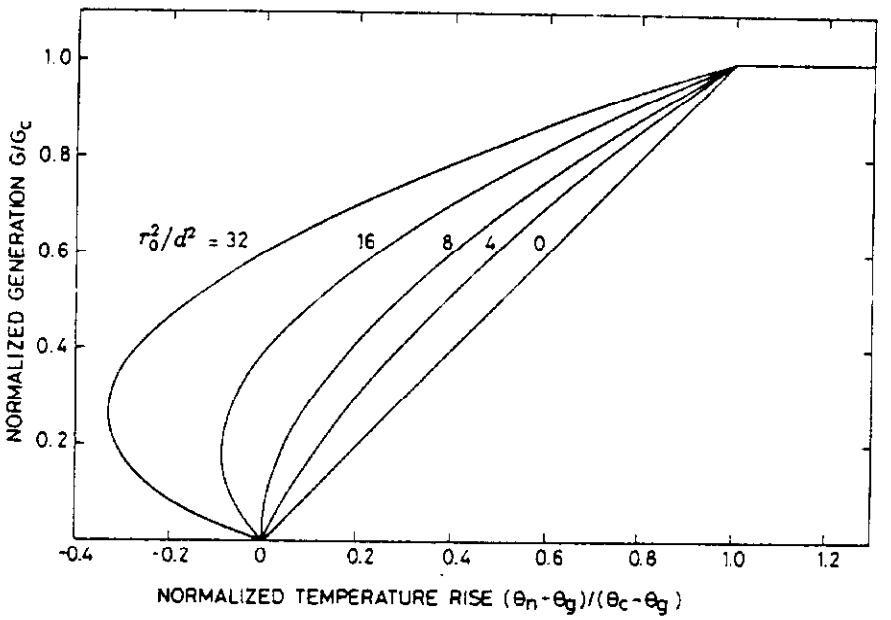

Fig. 18. Generation in a composite strand containing superconductor in the shape of cylindrical filaments as a function of copper temperature θ_n.

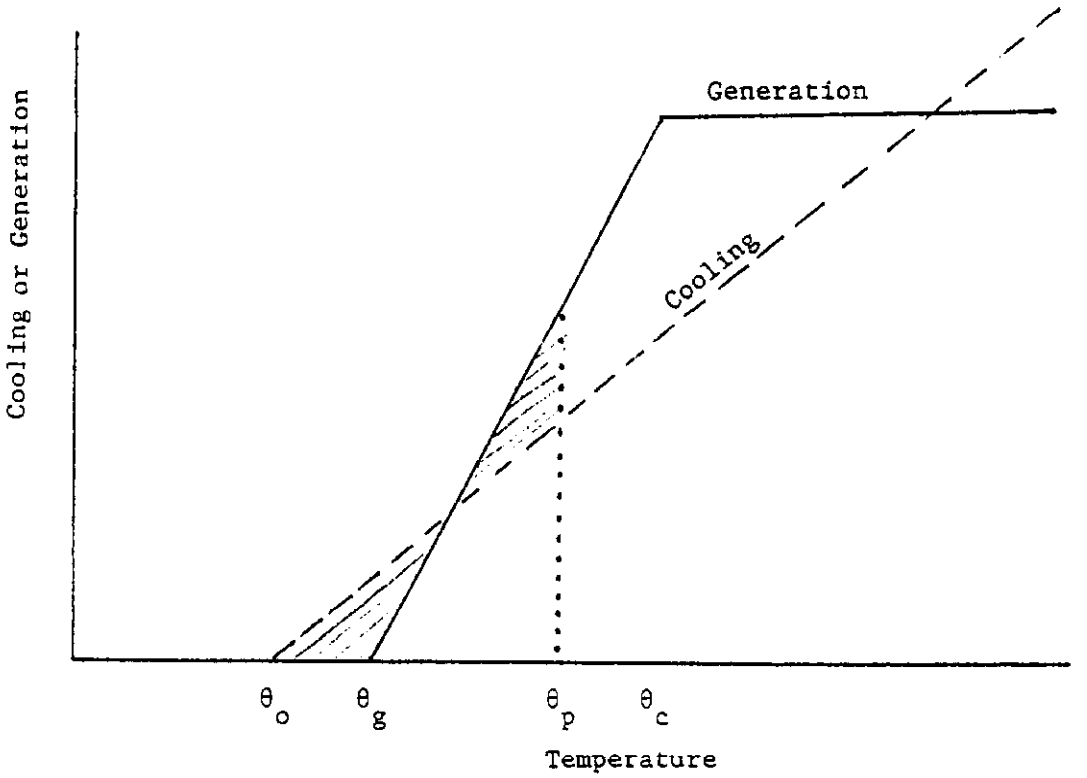

Fig. 19. To satisfy the equal-area theorem, θ_p need not be the intersection of the cooling and power generation curve. Sometimes, θ_p is not even the peak temperature.